Title
A High-Diversity Transceiver Design for MISO Broadcast Channels

Journal
IEEE Transactions on Wireless Communications, 18(5)

ISSN
1536-1276

Authors
Seo, Junyeong
Sung, Youngchul
Jafarkhani, Hamid

Publication Date
2019-05-01

DOI
10.1109/twc.2019.2905609

A High-Diversity Transceiver Design for K-User MISO Broadcast Channels

Junyeong Seo, *Student Member, IEEE*, Youngchul Sung†, *Senior Member, IEEE*, and Hamid Jafarkhani, *Fellow, IEEE*

Abstract

In this paper, a new transceiver architecture is proposed for K-user multiple-input single-output (MISO) broadcast channels (BCs) to overcome the drawback of the conventional linear zero-forcing (ZF) downlink beamforming. The proposed transceiver architecture is based on channel-adaptive user grouping and mixture of linear and nonlinear reception: it groups users with closely-aligned channels and applies superposition coding and successive interference cancellation (SIC) decoding to each group composed of users with closely-aligned channels, while applying ZF beamforming across roughly-orthogonal user groups. The outage probability and diversity order of the proposed transceiver architecture are analyzed based on newly derived closed-form lower bounds on the achievable rates of a general multi-user (MU) MISO BC with superposition coding and SIC decoding and the property of the proposed user grouping algorithm. It is shown that the proposed transceiver architecture can achieve the diversity order of the single-user maximum ratio transmit (MRT) beamforming. Hence, the proposed transceiver architecture can provide much higher diversity order and more reliable communication compared to the conventional ZF downlink beamforming under channel fading environments. Numerical results validate our analysis and show the superiority of the proposed scheme over the conventional ZF downlink beamforming in outage performance.

Index Terms

K-user MISO broadcast channels, outage probability, diversity order, successive interference cancellation, user grouping, mixture reception, zero-forcing beamforming

†Corresponding author

J. Seo and Y. Sung are with Dept. of Electrical Engineering, KAIST, Daejeon 305-701, South Korea, and H. Jafarkhani is with Center for Pervasive Communications & Computing, UC Irvine, CA, USA. E-mail: jyseo@kaist.ac.kr, ysung@ee.kaist.ac.kr, and hamidj@uci.edu. This work was supported in part by Basic Science Research Program through the National Research Foundation of Korea (NRF) funded by the Ministry of Education (2013R1A1A2A10060852) and supported in part by the NSF Award CCF-1526780.

I. Introduction

The MU-MISO BC model is an important channel model which captures modern cellular downlink communication in which a base station (BS) equipped with multiple transmit antennas simultaneously serves multiple receivers each equipped with a single receive antenna at the same time-and-frequency resource block by using the spatial domain. Due to its importance it has been investigated extensively for more than a decade and major current wireless communication standards support MU-MISO BC downlink communication [1]–[5]. It is known that the capacity region of a MU-MISO BC can be achieved by dirty paper coding (DPC) [2]. However, because of the unavailability of practical dirty paper codes, simple linear downlink beamforming such as ZF beamforming is widely considered and used in practice [4], [6]. Although such simple linear beamforming is not a capacity-achieving scheme, it can yield good performance when it is combined with multi-user diversity and user scheduling [3], [4], [7]–[9]. That is, when the number of users in the cell is sufficiently large as compared to the number N of transmit antennas, the BS can select N users with nearly orthogonal channel vectors so that linear ZF downlink beamforming is sufficient. However, such orthogonality-based user scheduling for linear downlink beamforming may not be appropriate in certain cases. One example is the case in which the number of transmit antennas is large under rich scattering environments, since it is difficult to simultaneously select multiple users with roughly orthogonal channels in this case [8]–[10]. Thus, for a MU-MISO BC with a large number of transmit antennas it was proposed that the BS selects the users for simultaneous service arbitrarily and applies linear ZF beamforming [10]. Another emerging important example is *ultra-reliable low-latency communication (URLLC)* for fast machine-type communication and control in 5G [11]. In the case of URLLC, such orthogonality-based user scheduling induces extra delay in communication, since the users requiring immediate data transmission may not have channel vectors nearly orthogonal to each other or to other on-going overlapping data users under spatial multiplexing, and these immediate-communication-requiring users may not be scheduled simultaneously by such orthogonality-based user scheduling. Hence, it is preferred that in this case the BS immediately schedules the users requiring low-latency data transmission regardless of their channel vectors' mutual orthogonality. In both examples, the channel vectors of the scheduled users are not guaranteed to be nearly orthogonal and the performance of linear ZF beamforming can be severely degraded since the channel vectors of some of the scheduled users can be closely aligned and the channel alignment causes poor conditioning of the channel matrix for ZF inversion.

In this paper, hinted by the fact that non-linear processing is required for optimal operation for K-

user MISO BCs and motivated by the recent interest in superposition coding and SIC decoding for non-orthogonal multiple access (NOMA) [12], [13], we propose a new transceiver architecture for K-user MISO BCs to overcome the drawback of the fully linear ZF downlink beamforming, based on *channel-adaptive user grouping* and *mixture of linear and non-linear reception*. The basic idea of the proposed transceiver architecture is as follows. Under the assumption of independent and identically distributed (i.i.d.) realization of K channel vectors in a K-user MISO BC, if the channel vectors of some users are closely aligned, the performance of ZF beamforming is severely degraded. However, if we group the closely-aligned users and apply superposition coding and non-linear SIC decoding for each closely-aligned user group while applying ZF beamforming across roughly-orthogonal user-groups, the performance degradation by the full ZF beamforming can be alleviated. Preliminary study on such user grouping and mixture transreception was performed on the two-user grouping case, where intra-group rate analysis is rather simple, in [14], [15]. In [15], Pareto-optimal beam design is considered for the two-user grouping case, the beam vectors and corresponding rates are numerically obtained, and the performance of a mixture reception scheme is compared with the full ZF beamforming numerically. In [14], under the assumption of two users in each group, closed-form beam vectors are obtained to minimize the transmit power under a signal-to-interference-plus-noise ratio (SINR) constraint for each user based on quasi-degradation, and it was shown that such a mixture architecture based on two-user grouping increases the diversity order by one as compared to the conventional ZF downlink beamforming. Although such two-user grouping for the mixture transceiver architecture is tractable, it has limitation in diversity order improvement. The related idea of the hierarchical coding and grouping users, in the dual scenario of multiple access channel, has been discussed in [16].

In this paper, we fully generalize the mixture transceiver architecture for general K-user MISO BCs, based on adaptive user grouping. In the proposed new mixture architecture, the number of members in each group is not fixed as two but depends on channel realization. To enable analysis of the outage probability and diversity order of the proposed mixture transceiver architecture, we derive a new lower bound on the achievable rate of each user in closed form in terms of each user's channel norm for a MU-MISO BC with superposition coding and SIC decoding with an arbitrary number of users (not limited as two). Combining the newly derived achievable rate result and the property of the proposed user grouping algorithm, we derive the diversity order of the proposed transceiver architecture, and show that *the proposed transceiver architecture can achieve the diversity order of the single-user MRT beamforming* and thus can yield much higher diversity order and more reliable communication for MU-MISO downlink compared to the conventional ZF downlink beamforming under channel fading environments.

Notations: Vectors and matrices are written in boldface with matrices in capitals. All vectors are column vectors. For a matrix $\mathbf{A}$, $\mathbf{A}^*$, $\mathbf{A}^H$, $\mathbf{A}^T$ and $\text{Tr}(\mathbf{A})$ indicate the complex conjugate, conjugate transpose, transpose and trace of $\mathbf{A}$, respectively, and $\mathcal{C}(\mathbf{A})$ and $\mathcal{C}^{\perp}(\mathbf{A})$ denotes the linear subspace spanned by the columns of $\mathbf{A}$ and its orthogonal complement, respectively. $\mathbf{\Pi_A}$ and $\mathbf{\Pi_A^{\perp}}$ are the projection matrices to $\mathcal{C}(\mathbf{A})$ and $\mathcal{C}^{\perp}(\mathbf{A})$, respectively. $[\mathbf{a}_1, \cdots, \mathbf{a}_n]$ denotes the matrix composed of column vectors $\mathbf{a}_1, \cdots, \mathbf{a}_n$. $||\mathbf{a}||$ represents the 2-norm of vector $\mathbf{a}$. $\mathbf{I}_n$ denotes the identity matrix of size n (the subscript is omitted when unnecessary). $\mathbf{x} \sim \mathcal{CN}(\boldsymbol{\mu}, \boldsymbol{\Sigma})$ means that random vector $\mathbf{x}$ is circularly-symmetric complex Gaussian distributed with mean vector $\boldsymbol{\mu}$ and covariance matrix $\boldsymbol{\Sigma}$.

II. The Channel Model and Preliminaries

A. The Channel Model

In this paper, we consider a K-user Gaussian MISO BC composed of a transmitter with N transmit antennas and K single-antenna users (i.e., receivers), where the number of users is less than or equal to the number of transmit antennas, i.e., $K \leq N$. The received signal y_k at the k-th user is given by

$$y_k = \mathbf{h}_k^H \mathbf{x} + n_k, \quad k = 1, 2, \cdots, K, \tag{1}$$

where $\mathbf{x}$ is the $N \times 1$ transmit signal vector at the transmitter with the total transmit power $P_t = \mathbb{E}\{\mathbf{x}\mathbf{x}^H\}$, n_k is the additive white Gaussian noise (AWGN) at the k-th user, i.e., $n_k \sim \mathcal{CN}(0, \sigma^2)$ with σ^2 set to 1 for simplicity, and $\mathbf{h}_k$ is the $N \times 1$ (conjugated) channel vector from the transmitter to the k-th user following independent Rayleigh fading,* i.e.,

$$\mathbf{h}_k = [h_{k1}, h_{k2}, \cdots, h_{kN}]^T \overset{i.i.d.}{\sim} \mathcal{CN}(\mathbf{0}, 2\mathbf{I}). \tag{2}$$

Concatenating all the received signals $y_1, \cdots, y_K$, we can write the matrix model for the received signals as

$$\mathbf{y} = \mathbf{H}^H \mathbf{x} + \mathbf{n}, \tag{3}$$

where $\mathbf{y} = [y_1, y_2, \cdots, y_K]^T$, $\mathbf{n} = [n_1, n_2, \cdots, n_K]^T$, and $\mathbf{H} = [\mathbf{h}_1, \mathbf{h}_2, \cdots, \mathbf{h}_K]$. Due to the assumption of $K \leq N$, the $K \times N$ overall channel matrix $\mathbf{H}^H$ is a fat matrix and hence it is right-invertible so that conventional ZF transmit beamforming is feasible. Design of the signal vector $\mathbf{x}$ and receiver processing based on $\{y_1, y_2, \cdots, y_K\}$ will be explained in the subsequent sections.

*We set $2\mathbf{I}$ as the covariance matrix for convenience so that both real and imaginary components of each element of $\mathbf{h}_k$ have variance one and thus $||\mathbf{h}_k||^2$ has the chi-square distribution of degrees of freedom $2N$. Different scaling can be absorbed into the transmit power.

B. Preliminaries: Reliability and Diversity Order

Channel fading is inherent in wireless communication, and communication reliability under channel fading is dependent on the diversity order of the communication channel. Consider the well-known single-user MRT beamforming with multiple transmit antennas. The corresponding channel model is given by the channel model (1) with only a single user, i.e., $K = 1$. For MRT beamforming, we have $\mathbf{x} = \frac{\mathbf{h}_1}{||\mathbf{h}_1||}\sqrt{p_1}s_1$ with $\mathbb{E}\{|s_1|^2\} = 1$. The resulting equivalent single-input single-output (SISO) channel and rate are respectively given by

$$y_1 = ||\mathbf{h}_1||\sqrt{p_1}s_1 + n_1 \quad \text{and} \quad R_1 = \log(1 + ||\mathbf{h}_1||^2\text{SNR}), \quad \text{SNR} := \frac{p_1}{\sigma^2}, \tag{4}$$

where the probability density function (pdf) of $||\mathbf{h}_1||^2 = |h_{11}|^2 + \cdots + |h_{1N}|^2$ is given by the chi-square distribution with degree of freedom $2N$, since it is the sum of the squares of $2N$ standard normal random variables:

$$f_{||\mathbf{h}_1||^2}(x) = \frac{1}{2^N(N-1)!}x^{N-1}e^{-x/2} = \frac{1}{2^N(N-1)!}x^{N-1} + o(x^{N-1}), \text{ as } x \to 0, \tag{5}$$

where $o(\cdot)$ is the small o notation. Communication outage is defined as the event that the channel cannot support a given target rate R^{th}, and the corresponding outage probability is given by $P_{out} = \Pr\{R_1 < R^{th}\}$ [17]. Then, the diversity of order of the channel is defined as [17]

$$D := -\lim_{\text{SNR}\to\infty} \frac{\log P_{out}}{\log \text{SNR}}. \tag{6}$$

In the single-user MRT beamforming case, the outage probability is given by [17]

$$P_{out} = \Pr\left\{||\mathbf{h}_1||^2 \le \frac{2^{R^{th}-1}}{\text{SNR}}\right\} \approx \frac{(2^{R^{th}} - 1)^N}{2^N N!\text{SNR}^N}, \tag{7}$$

and hence the diversity order in this case is given by N. That is, the outage probability decays as SNR^{-N}, as SNR increases. Note that in the case of a Rayleigh-fading SISO channel with a single transmit antenna $N = 1$, the pdf (5) reduces to

$$f_{|h_{11}|^2}(x) = \frac{1}{2}e^{-x/2}, \tag{8}$$

and the diversity order reduces to one. Hence, MRT beamforming with N transmit antennas increases the diversity order by N times as compared to the SISO case.

Now, consider the general K-user Gaussian MISO BC (1) with ZF downlink beamforming for $K = N$. In this ZF beamforming case, the overall transmit signal $\mathbf{x}$ is given by $\mathbf{x} = \mathbf{w}_1^{ZF}\sqrt{p_1}s_1 + \cdots +$

$\mathbf{w}_K^{ZF}\sqrt{p_K}s_K$, where $\mathbf{w}_k^{ZF}$ and s_k are the ZF beam vector and data symbol for the k-th user with $||\mathbf{w}_k^{ZF}||^2 = 1$ and $\mathbb{E}\{|s_k|^2\} = 1$, respectively. Here, the ZF beam vector $\mathbf{w}_k^{ZF}$ lies in $\mathcal{C}^{\perp}([\mathbf{h}_1, \cdots, \mathbf{h}_{k-1}, \mathbf{h}_{k+1}, \cdots, \mathbf{h}_K])$, i.e., the one-dimensional orthogonal space of the linear subspace spanned by the channel vectors $\mathbf{h}_1, \cdots, \mathbf{h}_{k-1}, \mathbf{h}_{k+1}, \cdots, \mathbf{h}_K$, so that $\mathbf{h}_i^H\mathbf{w}_k^{ZF} = 0$ for all $i \neq k$. Then, the resulting SISO channel for the k-th user is given by

$$y_k = \mathbf{h}_k^H\mathbf{w}_k^{ZF}\sqrt{p_k}s_k + n_k. \tag{9}$$

In the case of independent Rayleigh fading, the channel vector $\mathbf{h}_k$ and the remaining $\{\mathbf{h}_1, \cdots, \mathbf{h}_{k-1}, \mathbf{h}_{k+1}, \cdots, \mathbf{h}_K\}$ are independent. Hence, the one-dimensional subspace $\mathcal{C}^{\perp}([\mathbf{h}_1, \cdots, \mathbf{h}_{k-1}, \mathbf{h}_{k+1}, \cdots, \mathbf{h}_K])$ is also independent of $\mathbf{h}_k$, and hence $\mathbf{h}_k$ is circularly-symmetric Gaussian distributed over $\mathbb{C}^N$ with respect to a reference direction of $\mathcal{C}^{\perp}([\mathbf{h}_1, \cdots, \mathbf{h}_{k-1}, \mathbf{h}_{k+1}, \cdots, \mathbf{h}_K])$. Therefore, taking the inner product between $\mathbf{h}_k$ and the unit-norm vector $\mathbf{w}_k^{ZF} \in \mathcal{C}^{\perp}([\mathbf{h}_1, \cdots, \mathbf{h}_{k-1}, \mathbf{h}_{k+1}, \cdots, \mathbf{h}_K])$ is equivalent to taking only one component out of N complex Gaussian components, and thus $|\mathbf{h}_k^H\mathbf{w}_k^{ZF}|^2$ has the same pdf as (8). Hence, the corresponding diversity order for the k-th user is simply one for all k [14], as in the SISO Rayleigh fading channel. Thus, ZF downlink beamforming for K-user MISO BCs loses the diversity gain possibly obtainable from multiple transmit antennas, and is not desirable from the perspective of reliable communication under fading environments.

Note that if $\mathbf{h}_k$ is perfectly orthogonal to $\mathbf{h}_1, \cdots, \mathbf{h}_{k-1}, \mathbf{h}_{k+1}, \cdots, \mathbf{h}_K$, then $\mathcal{C}^{\perp}([\mathbf{h}_1, \cdots, \mathbf{h}_{k-1}, \mathbf{h}_{k+1}, \cdots, \mathbf{h}_K])$ is perfectly aligned with $\mathbf{h}_k$ and hence in this case we have

$$\mathbf{h}_k^H\mathbf{w}_k^{ZF} = ||\mathbf{h}_k||. \tag{10}$$

In this case, the resulting SISO channel for the k-th user is the same as that of the MRT beamforming single-user channel in (4). Furthermore, suppose that the angle between $\mathbf{h}_k$ and one-dimensional subspace $\mathcal{C}^{\perp}([\mathbf{h}_1, \cdots, \mathbf{h}_{k-1}, \mathbf{h}_{k+1}, \cdots, \mathbf{h}_K])$ is equal to or less than a certain fixed threshold α. Then, we have

$$|\mathbf{h}_k^H\mathbf{w}_k^{ZF}| \geq ||\mathbf{h}_k|| \cos\alpha. \tag{11}$$

Since $\cos\alpha$ is a constant, the pdf of $|\mathbf{h}_k^H\mathbf{w}_k^{ZF}|^2$ is a certain scaled version of that of $||\mathbf{h}_k||^2$ (the meaning of this statement will become clear in later sections), and the outage behavior for the k-th user in this case should be the same as that of the MRT single-user case as SNR increases without bound. Reflecting this, one can recognize that the degradation of diversity order of ZF beamforming for the K-user MISO BC with independent channel fading results from the uncontrolled and arbitrary angle between $\mathbf{h}_k$ and

$\mathcal{C}^{\perp}([\mathbf{h}_1, \cdots, \mathbf{h}_{k-1}, \mathbf{h}_{k+1}, \cdots, \mathbf{h}_K])$.

III. The Proposed Transceiver Architecture

In this section, motivated by the discussion in the previous section, we propose a new transceiver architecture for K-user Gaussian MISO BCs in order to enhance the diversity order of the resulting individual user channel under Rayleigh fading as compared to linear ZF downlink beamforming. The proposed architecture is based on adaptive user grouping, which enforces the ”angle” between the subspace of each group and the orthogonal complement of the union of all other groups' subspaces to be less than a certain threshold by grouping closely-aligned channel users as one group so that inter-group ZF beamforming does not harm the overall diversity order. On the other hand, to deal with users with closely-aligned channel vectors in each group, we apply superposition coding and SIC to the users in each group, since ZF beamforming cannot handle closely-aligned channel users without degrading the diversity order.

From here on, we explain the proposed transceiver architecture in detail. We consider the K-user MISO BC explained in Section II-A, as our channel model. We assume the following for our transceiver architecture:

A.1 (User Grouping): First, we group the K users into N_g groups. The constructed groups are denoted by the sets $\mathcal{G}_1, \mathcal{G}_2, \cdots, \mathcal{G}_{N_g}$ such that $\mathcal{G}_i \cap \mathcal{G}_j = \emptyset$ for $i \neq j$ and $\bigcup_{j=1}^{N_g} \mathcal{G}_j = \{1, 2, \cdots, K\}$. User grouping is adaptive in the sense that the number of groups can vary and the number of members in each group can vary from one to K, depending on the channels such that $\sum_{j=1}^{N_g} |\mathcal{G}_j| = K$. The constructed groups satisfy certain subspace angle properties in order to apply inter-group ZF beamforming without degrading the diversity order. The detailed method for user grouping will be presented in Section III-B.

A.2 (Inter-Group Beamforming): With the constructed groups, in order to control inter-group interference, we apply ZF beamforming across the constructed groups. With this inter-group ZF beamforming, the inter-group interference across the groups is zero.

A.3 (Intra-Group Processing: Superposition Coding and SIC): With the constructed groups, for intra-group processing we apply superposition coding and SIC decoding to each and every group with more than one user.

Under the aforementioned transceiver architecture, the transmit signal $\mathbf{x}$ of the transmitter can be expressed as

$$\mathbf{x} = \sum_{j=1}^{N_g} \mathbf{\Pi}^{(j)} \sum_{i \in \mathcal{G}_j} \sqrt{p_i^{(j)}} \mathbf{w}_i^{(j)} s_i^{(j)}, \tag{12}$$

where $s_i^{(j)}$ is the transmit symbol from $\mathcal{CN}(0,1)$ for User i in group $\mathcal{G}_j$, $\mathbf{w}_i^{(j)}$ is the $N \times 1$ intra-group beamforming vector for User i in group $\mathcal{G}_j$ out of the feasible set $\widetilde{\mathcal{W}} := \{\mathbf{w} \mid \|\mathbf{\Pi}^{(j)}\mathbf{w}\|^2 \leq 1\}$, $p_i^{(j)}$ is the power assigned to User i in group $\mathcal{G}_j$, and $\mathbf{\Pi}^{(j)}$ is the inter-group ZF projection matrix for group $\mathcal{G}_j$. We assume that the total transmit power P_t is divided such that $|\mathcal{G}_j| \times P_t/K$ is allocated to group $\mathcal{G}_j$. Then, from (1) the received signal at User i in group $\mathcal{G}_j$ can be written as

$$y_i^{(j)} = \mathbf{h}_i^{(j)H}\left(\mathbf{\Pi}^{(j)}\sum_{i\in\mathcal{G}_j}\sqrt{p_i^{(j)}}\mathbf{w}_i^{(j)}s_i^{(j)}\right) + n_i^{(j)} \overset{(a)}{=} \left(\mathbf{\Pi}^{(j)}\mathbf{h}_i^{(j)}\right)^H\left(\sum_{i\in\mathcal{G}_j}\sqrt{p_i^{(j)}}\mathbf{w}_i^{(j)}s_i^{(j)}\right) + n_i^{(j)}, \quad (13)$$

where $\mathbf{h}_i^{(j)}$ is the $N\times 1$ channel vector between the transmitter and User i in group $\mathcal{G}_j$, and $n_i^{(j)} \sim \mathcal{CN}(0,1)$ is the AWGN at User i in group $\mathcal{G}_j$ (here, the single user index k in (1) is properly mapped to the two indices, intra-group user index i and group index j). The inter-group ZF projection matrix $\mathbf{\Pi}^{(j)}$ is given by $\mathbf{\Pi}^{(j)} = \mathbf{\Pi}^{\perp}_{\tilde{\mathbf{H}}_j}$, where $\tilde{\mathbf{H}}_j$ is the matrix composed of all channel vectors except the channel vectors of the users in group $\mathcal{G}_j$, i.e.,

$$\tilde{\mathbf{H}}_j := [\mathbf{h}_1^{(1)}\cdots\mathbf{h}_{|\mathcal{G}_1|}^{(1)},\cdots,\mathbf{h}_1^{(j-1)}\cdots\mathbf{h}_{|\mathcal{G}_{j-1}|}^{(j-1)},\mathbf{h}_1^{(j+1)}\cdots\mathbf{h}_{|\mathcal{G}_{j+1}|}^{(j+1)},\cdots,\mathbf{h}_1^{(N_g)}\cdots\mathbf{h}_{|\mathcal{G}_{N_g}|}^{(N_g)}]. \quad (14)$$

Due to the inter-group ZF beamforming, there is no inter-group interference in (13), and the property of an orthogonal projection matrix, $(\mathbf{\Pi}^{\perp}_{\tilde{\mathbf{H}}_j})^H = \mathbf{\Pi}^{\perp}_{\tilde{\mathbf{H}}_j}$, is used in Step (a) in (13).

A. Intra-Group Beam Design and the Corresponding Rates

In this subsection, we consider intra-group beam vector design for the proposed transceiver architecture and analyze the achievable rates of the intra-group processing. First, consider each group $\mathcal{G}_j$ with one user. In this case, the received signal (13) reduces to

$$y_1^{(j)} = \left(\mathbf{\Pi}^{\perp}_{\tilde{\mathbf{H}}_j}\mathbf{h}_1^{(j)}\right)^H\sqrt{p_1^{(j)}}\mathbf{w}_1^{(j)}s_1^{(j)} + n_1^{(j)}, \quad |\mathcal{G}_j| = 1, \quad (15)$$

and the design of the intra-group beam vector $\mathbf{w}_1^{(j)}$ is simple. The optimal intra-group beam vector $\mathbf{w}_1^{(j)*}$ is the MRT beam matched to the projected effective channel vector $\mathbf{\Pi}^{\perp}_{\tilde{\mathbf{H}}_j}\mathbf{h}_1^{(j)}$, given by

$$\sqrt{p_1^{(j)}}\mathbf{w}_1^{(j)*} = \sqrt{P_t/K}\mathbf{\Pi}^{\perp}_{\tilde{\mathbf{H}}_j}\mathbf{h}_1^{(j)}/\|\mathbf{\Pi}^{\perp}_{\tilde{\mathbf{H}}_j}\mathbf{h}_1^{(j)}\|. \quad (16)$$

In this case, the optimal beam vector is equivalent to the ZF-beamforming vector with power P_t/K.

Next, consider the intra-group beam design for each group with more than one user. As aforementioned, we apply superposition coding and SIC in this case. Suppose that group $\mathcal{G}_j$ consists of L users ($L > 1$). Then, with the group index (j) omitted for convenience, the received signal for User i, $i = 1, \cdots, L$, in group $\mathcal{G}_j$ is given by

$$y_i = \mathbf{g}_i^H \left(\sum_{i=1}^{L} \sqrt{p_i} \mathbf{w}_i s_i \right) + n_i, \quad i = 1 \cdots, L, \tag{17}$$

where $\sum_{i=1}^{L} p_i \leq P$ with P being the total group power allocated to group $\mathcal{G}_j$ (i.e., $P = L \times P_t/K$), and $\mathbf{g}_i$ is the projected effective channel of User i given by

$$\mathbf{g}_i = \mathbf{\Pi}_{\tilde{\mathbf{H}}_j}^{\perp} \mathbf{h}_i^{(j)}, \quad i = 1, \cdots, L. \tag{18}$$

We assume that the intra-group beam vector $\mathbf{w}_i$ is designed based on the projected effective channels $\mathbf{g}_1, \cdots, \mathbf{g}_L$. Then, the feasible set for intra-group beam vector $\mathbf{w}_i$ is given by $\mathcal{W} := \{\mathbf{w} \mid \|\mathbf{w}\|^2 \leq 1\}$ from the fact that the beam design space for $\mathbf{w}_i$ is the linear subspace spanned by $\{\mathbf{g}_1, \cdots, \mathbf{g}_L\}$. (The beam component not in the subspace spanned by $\{\mathbf{g}_1, \cdots, \mathbf{g}_L\}$ does not affect the signal or the interference. Hence, it just wastes power.) Since $\mathbf{w}_i \in \mathcal{C}([\mathbf{g}_1, \cdots, \mathbf{g}_L])$, we have $\mathbf{w}_i \in \mathcal{C}^{\perp}(\tilde{\mathbf{H}}_j)$ by (18) and hence for the actual beam power constraint $\|\mathbf{\Pi}^{(j)} \mathbf{w}_i\|^2 \leq 1$, we have $\|\mathbf{\Pi}^{(j)} \mathbf{w}_i\|^2 = \|\mathbf{\Pi}_{\tilde{\mathbf{H}}_j}^{\perp} \mathbf{w}_i\|^2 = \|\mathbf{w}_i\|^2 \leq 1$ in this case. So, we have the feasible set $\mathcal{W}$ for $\mathbf{w}_i$.

Note that with inter-group ZF beamforming, the intra-group signal model is separated from group to group based on the projected effective channels, and the system model (17) is a conventional L-user MISO BC with superposition coding beamforming. For superposition coding and SIC, we assume that the in-group users are ordered according to their channel norms as $\|\mathbf{g}_1\|^2 \geq \|\mathbf{g}_2\|^2 \geq \cdots \geq \|\mathbf{g}_L\|^2$. With this assumption, SIC at the in-group receivers is applied such that User i decodes and cancels the interference from Users $L, L-1, \cdots, i+1$ sequentially. (Note that since User i has a better channel than Users $L, L-1, \cdots, i+1$, User i can decode the messages intended for Users $L, L-1, \cdots, i+1$.) Then, the rates of the in-group users can be expressed as

$$R_1 = \log_2 \left(1 + p_1 |\mathbf{g}_1^H \mathbf{w}_1|^2\right) \tag{19}$$

$$R_i = \log_2 \left(1 + \min\left\{\mathrm{SINR}_1^i, \cdots, \mathrm{SINR}_i^i\right\}\right), \quad i = 2, \cdots, L, \tag{20}$$

where SINR_j^i is the SINR when User j decodes the message intended for User i, given by

$$\mathrm{SINR}_j^i = \frac{p_i |\mathbf{g}_j^H \mathbf{w}_i|^2}{\sum_{m=1}^{i-1} p_m |\mathbf{g}_j^H \mathbf{w}_m|^2 + 1} \tag{21}$$

The achievable rate region $\mathcal{R}$ of the L-user MISO BC with superposition coding and SIC decoding is defined as the union of achievable rate-tuples:

$$\mathcal{R} := \bigcup_{\substack{(\mathbf{w}_1,\cdots,\mathbf{w}_L)\in\mathcal{W}^L \\ (p_1,\cdots,p_L)|p_i>0,\forall i,\ \sum_{i=1}^L p_i=P}} (R_1, R_2 \cdots, R_L), \tag{22}$$

where $(R_1, \cdots, R_L)$ is from (19) and (20). The Pareto boundary of the region $\mathcal{R}$ is the outer boundary of $\mathcal{R}$, and can be obtained by solving the following optimization problem:

$$\begin{aligned} \max_{\substack{\mathbf{w}_1,\cdots,\mathbf{w}_L \\ p_1,\cdots,p_L}} \quad & R_L \\ \text{subject to} \quad & R_i = R_i^*, \quad i = 1, \cdots L-1 \\ & \|\mathbf{w}_i\|^2 \leq 1, \quad i = 1, \cdots L \\ & \textstyle\sum_{i=1}^L p_i = P, \end{aligned} \tag{23}$$

where $(R_1^*, \cdots, R_{L-1}^*)$ is a rate-tuple of target rates of Users $1 \cdots, L-1$ out of the feasible target rate-tuple set. The optimization problem (23) was considered in [18], [19] in the context of NOMA. The problem (23) for given $(R_1^*, \cdots, R_{L-1}^*)$ can be solved by a convex programming approach based on reformulation [18] and the convex concave procedure (CCP) [20]. Therefore, if the feasible target rate-tuple set is known, one can design the beam vector $\mathbf{w}_1, \cdots, \mathbf{w}_L$ for the L-user MISO BC with superposition coding and SIC by first choosing the desired target rates of Users $1 \cdots, L-1$ from the feasible target rate-tuple set and next solving (23) to maximize R_L for given $(R_1^*, \cdots, R_{L-1}^*)$. However, difficulty lies in knowing the feasible target rate-tuple set for the L-user MISO BC with superposition coding and SIC since the rates depend on the beam vectors and channel vectors of all in-group users, although some induction approach for this was proposed in [19]. Most of all, the existing algorithms for the Pareto-optimal design problem (23) [18], [19] provide rates numerically based on numerically obtained beam vectors. Hence, these existing design algorithms do not provide closed-form rate expressions for general MU-MISO BCs with superposition coding and SIC decoding which is necessary for our analytical derivation of the diversity order. In order to circumvent this difficulty and obtain desired closed-form expressions on the achievable rates of the L-user MISO BC with superposition coding and SIC decoding, we consider beam design under the following constraint:

$$\begin{aligned} \mathbf{w}_1 &= \mathbf{w}_2 = \cdots = \mathbf{w}_L = \mathbf{w}, \quad ||\mathbf{w}||^2 \leq 1, \text{ i.e. } \mathbf{w} \in \mathcal{W} \\ p_i &= \delta_i P, \quad i = 1, 2, \cdots, L, \end{aligned} \tag{24}$$

where $(\delta_1, \cdots, \delta_L)$ is a power ratio-tuple out of the feasible power ratio-tuple set $\mathcal{D} := \{(\delta_1, \cdots, \delta_L) \mid \delta_i \geq$

$0\ \forall i,\ \sum_{i=1}^{L}\delta_i = 1\}$. Here, δ_i is the ratio of the total group power P to the power allocated to User i, i.e., $p_i = \delta_i P$ is assigned to User i. Note that the constraint (24) satisfies the original beam design constraint in (22). Based on the stricter constraint (24), the following proposition provides simple closed-form lower bounds on the achievable rates for the L-user MISO BC with superposition coding and SIC:

Proposition 1: In the L-user MISO BC (17) adopting superposition coding and SIC decoding with channel vectors $\mathbf{g}_1, \cdots, \mathbf{g}_L$ with ordering $\|\mathbf{g}_1\|^2 \geq \|\mathbf{g}_2\|^2 \geq \cdots \geq \|\mathbf{g}_L\|^2$ and total group power P, for an arbitrary given power ratio-tuple $(\delta_1, \cdots, \delta_L)$ out of the feasible power ratio-tuple set $\mathcal{D}$, the achievable rates $(R_1, R_2, \cdots, R_L)$ are lower bounded as

$$R_1 \geq \log_2\left(1 + \frac{1}{c}\delta_1\|\mathbf{g}_1\|^2 P\right) \tag{25}$$

$$R_i \geq \log_2\left(1 + \frac{\delta_i}{\sum_{m=1}^{i-1}\delta_m}\frac{1}{1 + \left(\frac{1}{c}\|\mathbf{g}_i\|^2\sum_{m=1}^{i-1}\delta_m P\right)^{-1}}\right), \quad i = 2, \cdots, L, \tag{26}$$

where the constant c is given by

$$c = \begin{cases} L & \text{if,} \quad L \leq 3, \\ 8L^2 & \text{if,} \quad L > 3. \end{cases} \tag{27}$$

Proof: See Appendix.

Note that unlike the target rate-tuple set $\{(R_1^*, \cdots, R_{L-1}^*)\}$ for the problem (23), the power ratio-tuple set $\mathcal{D}$ does not depend on the beam vectors and the channel vectors, and it is just a simplex. Thus, the rate lower bounds (25) and (26) with sweeping $(\delta_1, \cdots, \delta_L)$ within $\mathcal{D}$ yield an inner region of the achievable rate region $\mathcal{R}$ defined in (22). The key point in the derived lower bounds (25) and (26) on the achievable rates $(R_1, \cdots, R_L)$ is that *the lower bound on the rate R_i of User i in the superposition-and-SIC group is expressed only in terms of User i's channel norm square $||\mathbf{g}_i||^2$ and the power distribution factors* $(\delta_1, \cdots, \delta_L)$. This enables us to analyze the distribution of R_i via the distribution of $||\mathbf{g}_i||^2$ and to derive the diversity order of the proposed scheme in Section IV.

B. User Grouping

Now, we consider user grouping, which should be done properly for good performance of the proposed transceiver architecture. Since we apply inter-group ZF beamforming, a level of orthogonality across the constructed groups is required to guarantee high reliability, as discussed in Section II-B. Note that the channel orthogonality among the users within a group is not required, since superposition coding and SIC are applied to the users in each group. There can exist many user grouping methods that guarantee

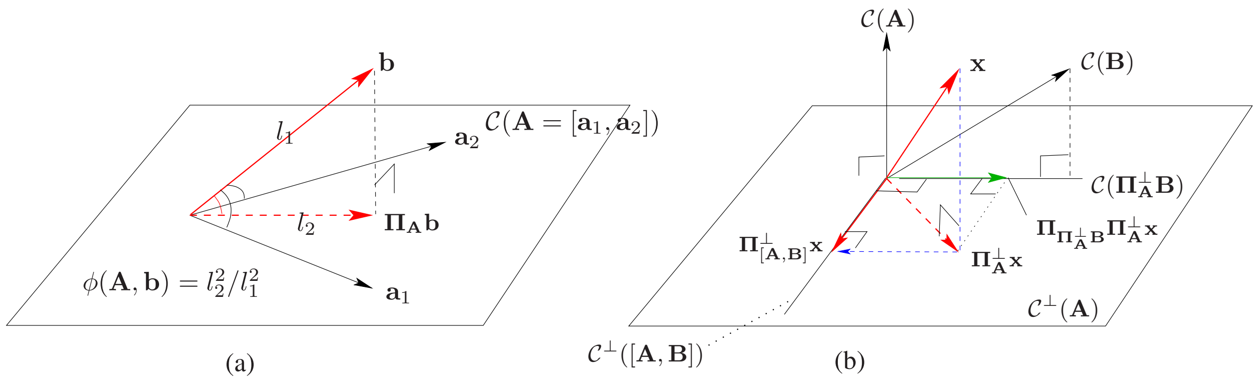

Fig. 1: (a) an illustration of $\phi(\mathbf{A}, \mathbf{b})$ and (b) an illustration of sequential orthogonal projection

certain orthogonality among the constructed groups. In this section, we provide one example for such user grouping. To measure the orthogonality across groups, we define a new subspace angle metric $\theta(\cdot, \cdot)$, which captures the angle between the subspaces $\mathcal{C}(\mathbf{A})$ and $\mathcal{C}(\mathbf{B})$ spanned by the columns of matrices $\mathbf{A}$ and $\mathbf{B}$, as

$$\theta(\mathbf{A}, \mathbf{B}) := \begin{cases} \max(\{\phi(\mathbf{A}, \mathbf{b}_i), \forall\ i\} \cup \{\phi(\mathbf{B}, \mathbf{a}_j), \forall\ j\}), & \text{if } \mathbf{A} \text{ and } \mathbf{B} \text{ are non-empty matrices} \\ 0, & \text{if } \mathbf{A} \text{ or } \mathbf{B} \text{ is an empty matrix,} \end{cases} \tag{28}$$

where $\mathbf{a}_i$ is the i-th column of $\mathbf{A}$, $\mathbf{b}_j$ is the j-th column of $\mathbf{B}$, and $\phi(\cdot, \cdot)$ is another newly-defined angle metric which captures the angle between the vector $\mathbf{b}$ and the subspace $\mathcal{C}(\mathbf{A})$, defined as

$$\phi(\mathbf{A}, \mathbf{b}) := \frac{\|\mathbf{A}(\mathbf{A}^H\mathbf{A})^{-1}\mathbf{A}^H\mathbf{b}\|^2}{\|\mathbf{b}\|^2}. \tag{29}$$

In case of $\mathbf{A} = [\mathbf{a}]$ is a vector, ϕ reduces to the square of the angle cosine of two vectors $\mathbf{a}$ and $\mathbf{b}$:

$$\phi(\mathbf{a}, \mathbf{b}) = \frac{|\mathbf{a}^H\mathbf{b}|^2}{\|\mathbf{a}\|^2\|\mathbf{b}\|^2} = \cos^2\angle(\mathbf{a}, \mathbf{b}) \ \in [0, 1]. \tag{30}$$

When $\mathbf{B} = [\mathbf{b}]$ in (28) is a vector, $\theta(\mathbf{A}, \mathbf{b})$ simply reduces to $\phi(\mathbf{A}, \mathbf{b})$ because $\phi(\mathbf{A}, \mathbf{b}) \geq \phi(\mathbf{b}, \mathbf{a}_j)$ for all j, i.e., the angle between $\mathbf{b}$ and $\mathcal{C}(\mathbf{A})$ is smaller than or equal to the angle between $\mathbf{b}$ and individual column $\mathbf{a}_j$ of $\mathbf{A}$, as illustrated in Fig. 1(a). When $\theta = 0$, two subspaces $\mathcal{C}(\mathbf{A})$ and $\mathcal{C}(\mathbf{B})$ are mutually orthogonal. When $\theta = 1$, on the other hand, there exists either at least a column of $\mathbf{A}$ contained in $\mathcal{C}(\mathbf{B})$ or at least a column of $\mathbf{B}$ contained in $\mathcal{C}(\mathbf{A})$. Thus, when $\theta = 1$, the two subspaces $\mathcal{C}(\mathbf{A})$ and $\mathcal{C}(\mathbf{B})$ are not separated.

The proposed user grouping algorithm based on $\theta(\cdot, \cdot)$ is presented in Algorithm 1. Before explaining the algorithm, we introduce a useful lemma regarding sequential orthogonal projection necessary to

Algorithm 1 : The Proposed User Grouping Algorithm

```
Initialization:
A threshold value θ^{th} ∈ (0,1) is given.
Initially set f_1 ··· , f_K as the actual channel vectors h_1, ··· , h_K of the K users.
Set 𝒦 ← {1, ··· , K} (initial candidate set)
Set i_g ← 0 (group index)
Set n_g ← 1 (number of users in group)
Set F_𝒦 ← [f_1, ··· , f_K].

Execution:
While n_g ≤ K
   Find a group of users {u_1^*, ··· , u_{n_g}^*} with cardinality n_g such that 𝒞(F_{u_1^*,···,u_{n_g}^*}) and
   𝒞(F_{𝒦\{u_1^*,···,u_{n_g}^*}}) satisfy
        θ(F_{𝒦\{u_1^*,···,u_{n_g}^*}}, F_{u_1^*,···,u_{n_g}^*}) ≤ θ^{th}.        (31)
      If we find such a group of users {u_1^*, ··· , u_{n_g}^*},
         i_g ← i_g + 1 (increase the group index by one).
         𝒢_{i_g} ← {u_1^*, ··· , u_{n_g}^*} (construct one group).
         𝒦 ← 𝒦 \ {u_1^*, ··· , u_{n_g}^*} (update 𝒦 by removing the selected users from the candidate set).
         Update the vector f_u as f_u ← (I − F_{𝒢_{i_g}} (F^H_{𝒢_{i_g}} F_{𝒢_{i_g}})^{-1} F^H_{𝒢_{i_g}}) f_u, ∀u ∈ updated 𝒦
         Construct new F_𝒦 with the updated f_u, ∀u ∈ updated 𝒦.
      Else
         n_g ← n_g + 1
      Endif
Endwhile
N_g ← i_g.
(Throughout the algorithm, F_𝒮 means the submatrix of current F_𝒦 composed of {current f_u, ∀u ∈
𝒮 ⊂ 𝒦}.)
```

explain the algorithm.

Lemma 1: For a vector $\mathbf{x}$ and matrices $\mathbf{A}$ and $\mathbf{B}$ such that $[\mathbf{A}, \mathbf{B}]$ is a tall matrix, the following equality holds

$$\mathbf{\Pi}^{\perp}_{[\mathbf{A},\mathbf{B}]}\mathbf{x} = (\mathbf{I} - \mathbf{\Pi}_{\mathbf{\Pi}^{\perp}_{\mathbf{A}}\mathbf{B}})\mathbf{\Pi}^{\perp}_{\mathbf{A}}\mathbf{x} = \mathbf{\Pi}^{\perp}_{\mathbf{A}}\mathbf{x} - \mathbf{\Pi}^{\perp}_{\mathbf{A}}\mathbf{B}[(\mathbf{\Pi}^{\perp}_{\mathbf{A}}\mathbf{B})^H\mathbf{\Pi}^{\perp}_{\mathbf{A}}\mathbf{B}]^{-1}(\mathbf{\Pi}^{\perp}_{\mathbf{A}}\mathbf{B})^H\mathbf{\Pi}^{\perp}_{\mathbf{A}}\mathbf{x}. \tag{32}$$

Proof: See Appendix.

Lemma 1 states that the projection of $\mathbf{x}$ onto the orthogonal space of $\mathcal{C}([\mathbf{A}, \mathbf{B}])$ can be accomplished in two steps first by projecting $\mathbf{x}$ onto the orthogonal space of $\mathcal{C}(\mathbf{A})$ and then by projecting this projected vector onto the orthogonal space of $\mathcal{C}(\mathbf{\Pi}_{\mathbf{A}}^{\perp}\mathbf{B})$ (not $\mathcal{C}(\mathbf{B})$), as illustrated in Fig. 1(b). By successively applying Lemma 1, we can obtain $\mathbf{\Pi}_{[\mathbf{A}_1,\mathbf{A}_2,\cdots,\mathbf{A}_n]}^{\perp}\mathbf{x}$ in a successive manner, where $[\mathbf{A}_1,\cdots,\mathbf{A}_n]$ is a tall matrix. That is, we first project $\mathbf{x}$ onto $\mathcal{C}^{\perp}(\mathbf{A}_1)$ to obtain $\mathbf{\Pi}_{\mathbf{A}_1}^{\perp}\mathbf{x}$, and project the subspace matrices $\mathbf{A}_2,\mathbf{A}_3,\cdots,\mathbf{A}_n$ onto $\mathcal{C}^{\perp}(\mathbf{A}_1)$ to obtain $\mathbf{\Pi}_{\mathbf{A}_1}^{\perp}\mathbf{A}_2,\mathbf{\Pi}_{\mathbf{A}_1}^{\perp}\mathbf{A}_3,\cdots,\mathbf{\Pi}_{\mathbf{A}_1}^{\perp}\mathbf{A}_n$. Then, we project $\mathbf{\Pi}_{\mathbf{A}_1}^{\perp}\mathbf{x}$ onto $\mathcal{C}^{\perp}(\mathbf{\Pi}_{\mathbf{A}_1}^{\perp}\mathbf{A}_2)$ to obtain $(\mathbf{I}-\mathbf{\Pi}_{\mathbf{\Pi}_{\mathbf{A}_1}^{\perp}\mathbf{A}_2})\mathbf{\Pi}_{\mathbf{A}_1}^{\perp}\mathbf{x}$, and also project $\mathbf{\Pi}_{\mathbf{A}_1}^{\perp}\mathbf{A}_3,\cdots,\mathbf{\Pi}_{\mathbf{A}_1}^{\perp}\mathbf{A}_n$ onto $\mathcal{C}^{\perp}(\mathbf{\Pi}_{\mathbf{A}_1}^{\perp}\mathbf{A}_2)$ to obtain $(\mathbf{I}-\mathbf{\Pi}_{\mathbf{\Pi}_{\mathbf{A}_1}^{\perp}\mathbf{A}_2})\mathbf{\Pi}_{\mathbf{A}_1}^{\perp}\mathbf{A}_3,\cdots,(\mathbf{I}-\mathbf{\Pi}_{\mathbf{\Pi}_{\mathbf{A}_1}^{\perp}\mathbf{A}_2})\mathbf{\Pi}_{\mathbf{A}_1}^{\perp}\mathbf{A}_n$. Furthermore, we project $(\mathbf{I}-\mathbf{\Pi}_{\mathbf{\Pi}_{\mathbf{A}_1}^{\perp}\mathbf{A}_2})\mathbf{\Pi}_{\mathbf{A}_1}^{\perp}\mathbf{x}$ onto $\mathcal{C}^{\perp}((\mathbf{I}-\mathbf{\Pi}_{\mathbf{\Pi}_{\mathbf{A}_1}^{\perp}\mathbf{A}_2})\mathbf{\Pi}_{\mathbf{A}_1}^{\perp}\mathbf{A}_3)$, and project the remaining subspace matrices $(\mathbf{I}-\mathbf{\Pi}_{\mathbf{\Pi}_{\mathbf{A}_1}^{\perp}\mathbf{A}_2})\mathbf{\Pi}_{\mathbf{A}_1}^{\perp}\mathbf{A}_4,\cdots,(\mathbf{I}-\mathbf{\Pi}_{\mathbf{\Pi}_{\mathbf{A}_1}^{\perp}\mathbf{A}_2})\mathbf{\Pi}_{\mathbf{A}_1}^{\perp}\mathbf{A}_n$ correspondingly. We continue this process until step n is reached. Then, this gives us $\mathbf{\Pi}_{[\mathbf{A}_1,\mathbf{A}_2,\cdots,\mathbf{A}_n]}^{\perp}\mathbf{x}$.

Algorithm 1 tries to find single-user groups first (line 6). If the algorithm cannot find any single-user group further, it increases the number of users in group to two (lines 17 and 18), and tries to find two-user groups. It continues this process until n_g becomes K (line 9). Suppose that no group is found up to $n_g = K-1$. Then, at $n_g = K$, one argument in $\theta(\cdot,\cdot)$ in (31) becomes an empty matrix, θ becomes zero by the definition (28), and hence the condition (31) is satisfied. Thus, in this case the whole set $\{1,2,\cdots,K\}$ becomes a single group. Let us explain Algorithm 1 by using a specific example below:

Example 1: Suppose that initial $\mathcal{K}=\{1,2,3,4,5,6,7\}$ and suppose that initially user 1 satisfies $\theta([\mathbf{h}_2,\cdots,\mathbf{h}_7],\mathbf{h}_1)\le\theta^{th}$. Then, we update $\mathcal{G}_1=\{1\}$ (line 13) and $\mathcal{K}=\{2,3,4,5,6,7\}$ (line 14), and project the channel vectors $\mathbf{h}_2,\cdots,\mathbf{h}_7$ onto $\mathcal{C}^{\perp}([\mathbf{h}_1])$ to obtain the projected channel vectors $\mathbf{\Pi}_{\mathbf{h}_1}^{\perp}\mathbf{h}_2,\cdots,$ $\mathbf{\Pi}_{\mathbf{h}_1}^{\perp}\mathbf{h}_7$ (line 15). Next, suppose that $\theta([\mathbf{\Pi}_{\mathbf{h}_1}^{\perp}\mathbf{h}_3,\cdots,\mathbf{\Pi}_{\mathbf{h}_1}^{\perp}\mathbf{h}_7],\mathbf{\Pi}_{\mathbf{h}_1}^{\perp}\mathbf{h}_2)\le\theta^{th}$. (Note that at this point we compute $\theta(\cdot,\cdot)$ using the *projected* channels (lines 15 and 16).) Then, we update $\mathcal{G}_2=\{2\}$ and $\mathcal{K}=\{3,4,5,6,7\}$ and project $\mathbf{\Pi}_{\mathbf{h}_1}^{\perp}\mathbf{h}_3,\cdots,\mathbf{\Pi}_{\mathbf{h}_1}^{\perp}\mathbf{h}_7$ onto $\mathcal{C}^{\perp}(\mathbf{\Pi}_{\mathbf{h}_1}^{\perp}\mathbf{h}_2)$ to obtain the further projected channels $(\mathbf{I}-\mathbf{\Pi}_{\mathbf{\Pi}_{\mathbf{h}_1}^{\perp}\mathbf{h}_2})\mathbf{\Pi}_{\mathbf{h}_1}^{\perp}\mathbf{h}_3,\cdots,(\mathbf{I}-\mathbf{\Pi}_{\mathbf{\Pi}_{\mathbf{h}_1}^{\perp}\mathbf{h}_2})\mathbf{\Pi}_{\mathbf{h}_1}^{\perp}\mathbf{h}_7$. Now, suppose that we cannot find a single-user group further and that at $n_g=2$ only one pair of users $\{3,4\}$ satisfies $\theta([(\mathbf{I}-\mathbf{\Pi}_{\mathbf{\Pi}_{\mathbf{h}_1}^{\perp}\mathbf{h}_2})\mathbf{\Pi}_{\mathbf{h}_1}^{\perp}\mathbf{h}_5,\cdots,(\mathbf{I}-\mathbf{\Pi}_{\mathbf{\Pi}_{\mathbf{h}_1}^{\perp}\mathbf{h}_2})\mathbf{\Pi}_{\mathbf{h}_1}^{\perp}\mathbf{h}_7],[(\mathbf{I}-\mathbf{\Pi}_{\mathbf{\Pi}_{\mathbf{h}_1}^{\perp}\mathbf{h}_2})\mathbf{\Pi}_{\mathbf{h}_1}^{\perp}\mathbf{h}_3,(\mathbf{I}-\mathbf{\Pi}_{\mathbf{\Pi}_{\mathbf{h}_1}^{\perp}\mathbf{h}_2})\mathbf{\Pi}_{\mathbf{h}_1}^{\perp}\mathbf{h}_4])\le\theta^{th}$. Then, we update $\mathcal{G}_3=\{3,4\}$ and $\mathcal{K}=\{5,6,7\}$, and the further projected channels for users $\{5,6,7\}$ are obtained by projecting $(\mathbf{I}-\mathbf{\Pi}_{\mathbf{\Pi}_{\mathbf{h}_1}^{\perp}\mathbf{h}_2})\mathbf{\Pi}_{\mathbf{h}_1}^{\perp}\mathbf{h}_5,\cdots,(\mathbf{I}-\mathbf{\Pi}_{\mathbf{\Pi}_{\mathbf{h}_1}^{\perp}\mathbf{h}_2})\mathbf{\Pi}_{\mathbf{h}_1}^{\perp}\mathbf{h}_7$ onto $\mathcal{C}^{\perp}([(\mathbf{I}-\mathbf{\Pi}_{\mathbf{\Pi}_{\mathbf{h}_1}^{\perp}\mathbf{h}_2})\mathbf{\Pi}_{\mathbf{h}_1}^{\perp}\mathbf{h}_3,(\mathbf{I}-\mathbf{\Pi}_{\mathbf{\Pi}_{\mathbf{h}_1}^{\perp}\mathbf{h}_2})\mathbf{\Pi}_{\mathbf{h}_1}^{\perp}\mathbf{h}_4])$. These final projected channels for users $\{5,6,7\}$ are the same as the ZF projected channels $\mathbf{\Pi}_{[\mathbf{h}_1,\cdots,\mathbf{h}_4]}^{\perp}\mathbf{h}_5,\cdots,$ $\mathbf{\Pi}_{[\mathbf{h}_1,\cdots,\mathbf{h}_4]}^{\perp}\mathbf{h}_7$ by Lemma 1. At the next iteration, n_g becomes 3 since we assumed that there is no further two-user group; one argument of $\theta(\cdot,\cdot)$ becomes an empty matrix since $\mathcal{K}=\{5,6,7\}$ and $n_g=3$; hence $\mathcal{G}_4=\{5,6,7\}$; no user is left in the candidate set $\mathcal{K}$ after update (line 14); no further channel projection in line 15 occurs since updated $\mathcal{K}=\emptyset$; and the algorithm stops.

Now, let us consider the norm property of the projected ZF channels associated with the constructed groups in the example, which is the key aspect of the proposed user grouping algorithm. Consider user 1 in firstly-constructed $\mathcal{G}_1$. Since $\theta([\mathbf{h}_2, \cdots, \mathbf{h}_7], \mathbf{h}_1) \leq \theta^{th}$, by the definition of $\theta(\cdot,\cdot)$ in (28), we have

$$\phi(\tilde{\mathbf{H}}_1 = [\mathbf{h}_2, \cdots, \mathbf{h}_7], \mathbf{h}_1) = \frac{\|\tilde{\mathbf{H}}_1(\tilde{\mathbf{H}}_1^H\tilde{\mathbf{H}}_1)^{-1}\tilde{\mathbf{H}}_1^H\mathbf{h}_1\|^2}{\|\mathbf{h}_1\|^2} \leq \theta^{th} \tag{33}$$

Hence, we have

$$\begin{aligned} ||\mathbf{\Pi}^{\perp}_{\tilde{\mathbf{H}}_1}\mathbf{h}_1||^2 &= ||(\mathbf{I} - \tilde{\mathbf{H}}_1(\tilde{\mathbf{H}}_1^H\tilde{\mathbf{H}}_1)^{-1}\tilde{\mathbf{H}}_1^H)\mathbf{h}_1||^2 \\ &= (1 - \phi(\tilde{\mathbf{H}}_1, \mathbf{h}_1))||\mathbf{h}_1||^2 \text{ by Pythagorean theorem} \\ &\geq (1 - \theta^{th})||\mathbf{h}_1||^2. \end{aligned}$$

Next, consider the norm of the ZF effective channel for User 2 in $\mathcal{G}_2$. Due to the construction of $\mathcal{G}_1$ based on (33), $\mathbf{h}_1$ and $\mathbf{h}_2$ satisfy the following:

$$\begin{aligned} ||\mathbf{\Pi}^{\perp}_{\mathbf{h}_1}\mathbf{h}_2||^2 &= (1 - \phi(\mathbf{h}_1, \mathbf{h}_2))||\mathbf{h}_2||^2 \\ &\geq (1 - \phi(\tilde{\mathbf{H}}_1, \mathbf{h}_1))||\mathbf{h}_2||^2, \quad \text{since } \tilde{\mathbf{H}}_1 \text{ includes } \mathbf{h}_2 \\ &\geq (1 - \theta^{th})||\mathbf{h}_2||^2. \end{aligned} \tag{34}$$

By Lemma 1, $\mathbf{\Pi}^{\perp}_{[\mathbf{h}_1,\mathbf{h}_3,\cdots,\mathbf{h}_7]}\mathbf{h}_2$ can be obtained by sequential orthogonal projection as

$$\mathbf{\Pi}^{\perp}_{[\mathbf{h}_1,\mathbf{h}_3,\cdots,\mathbf{h}_7]}\mathbf{h}_2 = (\mathbf{I} - \mathbf{\Pi}_{[\mathbf{\Pi}^{\perp}_{\mathbf{h}_1}\mathbf{h}_3,\cdots,\mathbf{\Pi}^{\perp}_{\mathbf{h}_1}\mathbf{h}_7]})\mathbf{\Pi}^{\perp}_{\mathbf{h}_1}\mathbf{h}_2,$$

but $\mathcal{G}_2$ was constructed such that $\mathbf{\Pi}^{\perp}_{\mathbf{h}_1}\mathbf{h}_2$ and $[\mathbf{\Pi}^{\perp}_{\mathbf{h}_1}\mathbf{h}_3, \cdots, \mathbf{\Pi}^{\perp}_{\mathbf{h}_1}\mathbf{h}_7]$ satisfy the threshold θ^{th} requirement. Combining this fact and (34), we have

$$||\mathbf{\Pi}^{\perp}_{[\mathbf{h}_1,\mathbf{h}_3,\cdots,\mathbf{h}_7]}\mathbf{h}_2||^2 \geq (1 - \theta^{th})^2||\mathbf{h}_2||^2.$$

Then, consider User 3 in $\mathcal{G}_3 = \{3, 4\}$. (The same applies to User 4 in $\mathcal{G}_3$.) By Lemma 1, we have

$$\mathbf{\Pi}^{\perp}_{[\mathbf{h}_1,\mathbf{h}_2]}\mathbf{h}_3 = (\mathbf{I} - \mathbf{\Pi}_{\mathbf{\Pi}^{\perp}_{\mathbf{h}_1}\mathbf{h}_2})\mathbf{\Pi}^{\perp}_{\mathbf{h}_1}\mathbf{h}_3 \tag{35}$$

$$\mathbf{\Pi}^{\perp}_{[\mathbf{h}_1,\mathbf{h}_2,\mathbf{h}_5,\mathbf{h}_6,\mathbf{h}_7]}\mathbf{h}_3 = (\mathbf{I} - \mathbf{\Pi}_{[\mathbf{\Pi}^{\perp}_{[\mathbf{h}_1,\mathbf{h}_2]}\mathbf{h}_5,\mathbf{\Pi}^{\perp}_{[\mathbf{h}_1,\mathbf{h}_2]}\mathbf{h}_6,\mathbf{\Pi}^{\perp}_{[\mathbf{h}_1,\mathbf{h}_2]}\mathbf{h}_7]})\mathbf{\Pi}^{\perp}_{[\mathbf{h}_1,\mathbf{h}_2]}\mathbf{h}_3. \tag{36}$$

In (35), $\mathcal{G}_1 = \{1\}$ was constructed such that $\mathbf{h}_1$ and $\mathbf{h}_3$ satisfy the angle constraint, and $\mathcal{G}_2 = \{2\}$ was constructed such that $\mathbf{\Pi}^{\perp}_{\mathbf{h}_1}\mathbf{h}_2$ and $\mathbf{\Pi}^{\perp}_{\mathbf{h}_1}\mathbf{h}_3$ satisfy the angle constraint. Hence, we have $||\mathbf{\Pi}^{\perp}_{\mathbf{h}_1}\mathbf{h}_3||^2 \geq (1 - \theta^{th})^2||\mathbf{h}_3||^2$. Furthermore, in (36), $\mathcal{G}_3 = \{3, 4\}$ was constructed such that $[\mathbf{\Pi}^{\perp}_{[\mathbf{h}_1,\mathbf{h}_2]}\mathbf{h}_3, \mathbf{\Pi}^{\perp}_{[\mathbf{h}_1,\mathbf{h}_2]}\mathbf{h}_4]$

and the remaining $[\mathbf{\Pi}^{\perp}_{[\mathbf{h}_1,\mathbf{h}_2]}\mathbf{h}_5, \mathbf{\Pi}^{\perp}_{[\mathbf{h}_1,\mathbf{h}_2]}\mathbf{h}_6, \mathbf{\Pi}^{\perp}_{[\mathbf{h}_1,\mathbf{h}_2]}\mathbf{h}_7]$ satisfy the angle constraint. Combining these facts, we have

$$||\mathbf{\Pi}^{\perp}_{[\mathbf{h}_1,\mathbf{h}_2,\mathbf{h}_5,\mathbf{h}_6,\mathbf{h}_7]}\mathbf{h}_k||^2 \geq (1-\theta^{th})^3||\mathbf{h}_k||^2, \quad k = 3, 4. \tag{37}$$

Finally, consider the norm of the ZF effective channels $\mathbf{\Pi}^{\perp}_{[\mathbf{h}_1,\cdots,\mathbf{h}_4]}\mathbf{h}_5, \cdots, \mathbf{\Pi}^{\perp}_{[\mathbf{h}_1,\cdots,\mathbf{h}_4]}\mathbf{h}_7$ of the last group $\mathcal{G}_4 = \{5, 6, 7\}$. These vectors are obtained by three sequential orthogonal projections based on Lemma 1, and at each projection stage the threshold θ^{th} was kept for group splitting. Hence, we have

$$||\mathbf{\Pi}^{\perp}_{[\mathbf{h}_1,\cdots,\mathbf{h}_4]}\mathbf{h}_k||^2 \geq (1-\theta^{th})^3||\mathbf{h}_k||^2, \; k = 5, 6, 7.$$

Note that in general the proposed user grouping algorithm satisfies the following norm reduction property for the ZF effective channels:

$$||\mathbf{g}_i^{(j)}||^2 = ||\mathbf{\Pi}^{\perp}_{\tilde{\mathbf{H}}_j}\mathbf{h}_i^{(j)}||^2 \geq (1-\theta^{th})^{N_g-1}||\mathbf{h}_i^{(j)}||^2, \tag{38}$$

where $\mathbf{\Pi}^{\perp}_{\tilde{\mathbf{H}}_j}$ is the ZF projection matrix for group $\mathcal{G}_j$, $\mathbf{h}_i^{(j)}$ is the channel vector of User i in group $\mathcal{G}_j$, and N_g is the number of constructed groups, which is bounded by K. Since the number of antennas, N, and the number of users, K $(\leq N)$, are fixed in our K-user MISO BC model with superposition coding and SIC, the lower bound $(1-\theta^{th})^{K-1} \in (0, 1)$ of $(1-\theta^{th})^{N_g-1}$ is a constant.

Now, let us define a useful quantity for further exposition: We define the degrees of freedom of a fading channel $\mathbf{h}$ as

$$d := \lim_{x\to 0}\frac{\log \Pr(\|\mathbf{h}\|^2 \leq x)}{\log x}. \tag{39}$$

This quantity captures the behavior of the tail probability of the random variable $||\mathbf{h}||^2$ in its lower tail, and the degrees of freedom d for $\mathbf{h}$ means that $\Pr(\|\mathbf{h}\|^2 \leq x)$ behaves as $x^d + o(x^d)$, as $x \to 0$. This quantity is directly related to the diversity order of the SISO communication channel with the channel gain $||\mathbf{h}||$. For example, a Rayleigh fading channel $\mathbf{h} \sim \mathcal{C}(\mathbf{0}, 2\mathbf{I}_N)$ has the degrees of freedom N since

$$\Pr(||\mathbf{h}||^2 \leq x) = \int_0^x f_{\|\mathbf{h}\|^2}(z)dz = \frac{1}{2^N N!}x^N + o(x^N), \text{ as } x \to 0 \tag{40}$$

and

$$\lim_{x\to 0}\frac{\log \Pr(\|\mathbf{h}\|^2 \leq x)}{\log x} = N, \tag{41}$$

where $f_{\|\mathbf{h}\|^2}(z)dz$ is given in (5). Finally, we provide the main statement of this subsection regarding the degrees of freedom of the ZF effective channels associated with the proposed grouping method in the following proposition:

Proposition 2: With the proposed transceiver architecture and the user grouping method in Algorithm 1, the projected effective channel $\mathbf{g}_j^{(i)} = \mathbf{\Pi}_{\tilde{\mathbf{H}}_j}^{\perp}\mathbf{h}_i^{(j)}$ in (13) resulting from inter-group ZF beamforming has the same degrees of freedom as the original channel $\mathbf{h}_i^{(j)}$, i.e.,

$$\lim_{x\to 0}\frac{\log \Pr(\|\mathbf{g}_i^{(j)}\|^2 \le x)}{\log x} = \lim_{x\to 0}\frac{\log \Pr(\|\mathbf{h}_i^{(j)}\|^2 \le x)}{\log x}, \quad \forall\ i,j. \tag{42}$$

Proof: See Appendix.

IV. Outage Analysis and Diversity Order of The Proposed Scheme

In this section, we present our main result of this paper regarding the diversity order of the proposed new transceiver architecture for K-user MISO BCs.

Theorem 1: For the K-user Gaussian MISO BC with N transmit antennas with independent Rayleigh fading described in Section II-A, let the channels be ordered as $\|\mathbf{h}_1\|^2 \ge \|\mathbf{h}_2\|^2 \cdots \ge \|\mathbf{h}_K\|^2$ and let the k-th user be the user with the k-th largest channel norm. Then, the diversity order for the k-th user achievable by the proposed transceiver architecture is given by

$$D_k = N \times (K - k + 1). \tag{43}$$

Here, the diversity order is defined as $D_k := \lim_{P_t\to\infty} -\frac{\log Pr\{R_k < R^{th}\}}{\log P_t}$, where R_k is the rate of the k-th user and R^{th} is a rate threshold. Note that $P_t \to \infty$ is equivalent to $\mathrm{SNR} = P_t/\sigma^2 \to \infty$ since we set the noise variance $\sigma^2 = 1$ for simplicity.

Proof: Proof is based on Propositions 1 and 2. In proof, we consider not only the distribution of the channel norm itself but also the order statistics resulting from the channel norm ordering. With the descending channel ordering $\|\mathbf{h}_1\|^2 \ge \|\mathbf{h}_2\|^2 \cdots \ge \|\mathbf{h}_K\|^2$, by order statistics the pdf of the k-th channel norm square is given by

$$f_{\|\mathbf{h}_k\|^2}(x) = \frac{K!}{(k-1)!(K-k)!}[F_{\|\mathbf{h}\|^2}(x)]^{K-k}[1 - F_{\|\mathbf{h}\|^2}(x)]^{k-1} f_{\|\mathbf{h}\|^2}(x) \tag{44}$$

where $f_{\|\mathbf{h}\|^2}(\cdot)$ and $F_{\|\mathbf{h}\|^2}$ are the pdf and cumulative distribution function (cdf) of chi-square distribution with degree of freedom $2N$:

$$f_{\|\mathbf{h}\|^2}(x) = \frac{1}{2^N(N-1)!}x^{N-1}e^{-x/2} = \frac{1}{2^N N!}x^{N-1} + o(x^{N-1}), \quad \text{as } x \to 0 \tag{45}$$

$$F_{\|\mathbf{h}\|^2}(x) = \frac{1}{2^N N!}x^N + o(x^N), \quad \text{as } x \to 0. \tag{46}$$

Hence, we have for the k-th largest channel norm square $||\mathbf{h}_k||^2$

$$f_{||\mathbf{h}_k||^2}(x) = c_k x^{N(K-k+1)-1} + o(x^{N(K-k+1)-1}), \quad \text{as } x \to 0, \tag{47}$$

and thus

$$\lim_{x\to 0} \frac{\log \Pr(\|\mathbf{h}_k\|^2 \le x)}{\log x} = N(K-k+1). \tag{48}$$

The outage probability of the k-th user is expressed as

$$\Pr(R_k < R^{th}) = \sum_{j=1}^{N_g} \left[\Pr(k \in \mathcal{G}_j) \cdot \Pr\left(R_k < R^{th} \middle| k \in \mathcal{G}_j \right) \right] \tag{49}$$

$$= \sum_{j=1}^{N_g} \Big[\Pr(k \in \mathcal{G}_j) \cdot \Big\{ \Pr\left(|\mathcal{G}_j| = 1 \mid k \in \mathcal{G}_j\right) \cdot \Pr\left(R_k < R^{th} \mid |\mathcal{G}_j| = 1, k \in \mathcal{G}_j \right)$$

$$+ \Pr(|\mathcal{G}_j| \ne 1 \mid k \in \mathcal{G}_j) \cdot \Pr\left(R_k < R^{th} \mid |\mathcal{G}_j| \ne 1, k \in \mathcal{G}_j \right) \Big\} \Big]. \tag{50}$$

i) Lower bound on the outage probability: We obtain a lower bound on the outage probability by considering only the event that the k-th user belongs to a group with cardinality one, i.e., the first term in the RHS of (50).

$$\Pr(R_k < R^{th}) \ge \sum_{j=1}^{N_g} \Pr(k \in \mathcal{G}_j) \cdot \Pr\left(|\mathcal{G}_j| = 1 \mid k \in \mathcal{G}_j\right) \cdot \Pr\left(R_k < R^{th} \,\middle|\, |\mathcal{G}_j| = 1, k \in \mathcal{G}_j \right)$$

$$= \sum_{j=1}^{N_g} \Pr\left(|\mathcal{G}_j| = 1, k \in \mathcal{G}_j\right) \cdot \Pr\left(R_k < R^{th} \,\middle|\, |\mathcal{G}_j| = 1, k \in \mathcal{G}_j \right)$$

$$= \sum_{j=1}^{N_g} \Pr\left(|\mathcal{G}_j| = 1, k \in \mathcal{G}_j\right) \cdot \Pr\left(\|\mathbf{\Pi}^{(j)} \mathbf{h}_k\|^2 < K \cdot (2^{R^{th}} - 1) \cdot P_t^{-1} \right), \tag{51}$$

where (51) holds due to the rate $R_k = \log(1 + P_t ||\mathbf{\Pi}^{(j)} \mathbf{h}_k||^2 / K)$ for a single-user group based on (15) and (16). Then, we have

$$-D_k = \lim_{P_t \to \infty} \frac{\log \Pr(R_k < R^{th})}{\log P_t} \tag{52}$$

$$\ge \lim_{P_t \to \infty} \frac{\log \left(\sum_{j=1}^{N_g} \left[\Pr\left(|\mathcal{G}_j| = 1, k \in \mathcal{G}_j\right) \cdot \Pr\left(\|\mathbf{\Pi}^{(j)} \mathbf{h}_k\|^2 < K \cdot (2^{R^{th}} - 1) \cdot P_t^{-1} \right) \right] \right)}{\log P_t} \tag{53}$$

$$= \lim_{P_t^{-1} \to 0} \frac{\log \left(\sum_{j=1}^{N_g} \left[\Pr\left(|\mathcal{G}_j| = 1, k \in \mathcal{G}_j\right) \cdot \Pr\left(\|\mathbf{\Pi}^{(j)} \mathbf{h}_k\|^2 < K \cdot (2^{R^{th}} - 1) \cdot P_t^{-1} \right) \right] \right)}{-\log P_t^{-1}} \tag{54}$$

$$= -N(K-k+1). \tag{55}$$

Here, (55) is valid because $||\mathbf{h}_k||^2$ has the channel order $N(K-k+1)$ by (47) and (48); the projected effective channel $\|\mathbf{\Pi}^{(j)}\mathbf{h}_k\|^2$ has the same channel order as $||\mathbf{h}_k||^2$ by Proposition 2; and the linear combination of terms with the same order has the same order as each term. Note that $\Pr\left(|\mathcal{G}_j|=1, k\in\mathcal{G}_j\right)$ depends only on the joint distribution of $(\mathbf{h}_1,\cdots,\mathbf{h}_k)$ for the given user grouping algorithm not on the power P_t.

ii) Upper bound on the outage probability:

For the upper bound, we need to include the second term in the RHS of (50) in addition to the first term in the RHS of (50) considered in the lower bound. The second term in the RHS of (50) is given by

$$\sum_{j=1}^{N_g}\Pr(k\in\mathcal{G}_j)\cdot\Pr\left(|\mathcal{G}_j|\neq 1 \mid k\in\mathcal{G}_j\right)\cdot\Pr\left(R_k<R^{th}\mid |\mathcal{G}_j|\neq 1, k\in\mathcal{G}_j\right) \tag{56}$$

$$=\sum_{j=1}^{N_g}\Pr\left(|\mathcal{G}_j|\neq 1, k\in\mathcal{G}_j\right)\cdot\Pr\left(R_k<R^{th}\mid |\mathcal{G}_j|\neq 1, k\in\mathcal{G}_j\right) \tag{57}$$

$$=\sum_{j=1}^{N_g}\sum_{\ell=2}^{K}\Pr\left(|\mathcal{G}_j|=\ell, k\in\mathcal{G}_j\right)\cdot\underbrace{\Pr\left(R_k<R^{th}\ \mid\ |\mathcal{G}_j|=\ell, k\in\mathcal{G}_j\right)}_{(a)}. \tag{58}$$

Define the following notations:

$$E_{k,j,i} := \text{Event that the } k\text{-th user is the } i\text{-th largest channel norm user in } \mathcal{G}_j \tag{59}$$

$$P_{k,j,i} := \Pr(E_{k,j,i}). \tag{60}$$

With these notations, the term (a) in (58) can be rewritten as

$$\Pr\left(R_k<R^{th}\ \Big|\ |\mathcal{G}_j|=\ell, k\in\mathcal{G}_j\right)=\sum_{i=1}^{\ell}P_{k,j,i}\cdot\Pr\left(R_k<R^{th}\ \Big|\ |\mathcal{G}_j|=\ell, k\in\mathcal{G}_j, E_{k,j,i}\right), \tag{61}$$

where R_k conditioned on the joint event $(|\mathcal{G}_j|=\ell, k\in\mathcal{G}_j, E_{k,j,i})$ is lower bounded by Proposition 1 as

$$R_k \geq \begin{cases} \log_2\left(1+\frac{1}{c}\delta_1^{(j)}\|\mathbf{\Pi}^{(j)}\mathbf{h}_k\|^2\frac{\ell P_t}{K}\right) & \text{if } i=1 \\ \log_2\left(1+\frac{\delta_i^{(j)}}{\sum_{m=1}^{i-1}\delta_m^{(j)}}\frac{1}{1+\left(\frac{1}{c}\|\mathbf{\Pi}^{(j)}\mathbf{h}_k\|^2\sum_{m=1}^{i-1}\delta_m^{(j)}\frac{\ell P_t}{K}\right)^{-1}}\right) & \text{if } i=2\cdots\ell. \end{cases} \tag{62}$$

where c is given in (27), and $(\delta_1^{(j)},\delta_2^{(j)},\cdots\delta_\ell^{(j)})$ is the power ratio-tuple in group $\mathcal{G}_j$, i.e., power $\delta_i^{(j)}\ell P_t/K$ is assigned to User i in group $\mathcal{G}_j$. ($\ell P_t/K$ is the total group power for group $\mathcal{G}_j$ with $|\mathcal{G}_j|=\ell$.) Therefore, the probability (61) is upper bounded as

$$\sum_{i=1}^{\ell}\left[P_{k,j,i}\cdot\Pr\left(R_k<R^{th}\;\middle|\;|\mathcal{G}_j|=\ell,k\in\mathcal{G}_j,E_{k,j,i}\right)\right] \tag{63}$$

$$\leq P_{k,j,1}\cdot\Pr\left(\log_2\left(1+\frac{1}{c}\delta_1^{(j)}\|\mathbf{\Pi}^{(j)}\mathbf{h}_k\|^2\frac{\ell P_t}{K}\right)<R^{th}\right)$$
$$+\sum_{i=2}^{\ell}\left[P_{k,j,i}\cdot\Pr\left(\log_2\left(1+\frac{\delta_i^{(j)}}{\sum_{m=1}^{i-1}\delta_m^{(j)}}\frac{1}{1+\left(\frac{1}{c}\|\mathbf{\Pi}^{(j)}\mathbf{h}_k\|^2\sum_{m=1}^{i-1}\delta_m^{(j)}\ell P_t/K\right)^{-1}}\right)<R^{th}\right)\right] \tag{64}$$

$$=P_{k,j,1}\cdot\Pr\left(\|\mathbf{\Pi}^{(j)}\mathbf{h}_k\|^2<(2^{R^{th}}-1)\cdot\frac{c}{\delta_1^{(j)}}\cdot\frac{K}{\ell}P_t^{-1}\right)$$
$$+\sum_{i=2}^{\ell}\left[P_{k,j,i}\cdot\Pr\left(\|\mathbf{\Pi}^{(j)}\mathbf{h}_k\|^2<c\left(\frac{\delta_i^{(j)}}{2^{R^{th}}-1}-\sum_{m=1}^{i-1}\delta_m^{(j)}\right)^{-1}\cdot\frac{K}{l}\cdot P_t^{-1}\right)\right], \tag{65}$$

where the threshold for $\|\mathbf{\Pi}^{(j)}\mathbf{h}_k\|^2$ in the second term in (65) is obtained by manipulation of the second term in (64). By Lemma 4 in Appendix, there always exists a collection of in-group power distribution factors $(\delta_1^{(j)},\cdots,\delta_\ell^{(j)})$ such that $(\frac{\delta_i^{(j)}}{2^{R^{th}}-1}-\sum_{m=1}^{i-1}\delta_m^{(j)})$ in (65) is strictly positive for all $i=2,\cdots,\ell$. Set $(\delta_1^{(j)},\cdots,\delta_\ell^{(j)})$ as one of such collections. Then, each probability term in (65) behaves as $P_t^{-N(K-k+1)}$ as $P_t\to\infty$, since $\|\mathbf{\Pi}^{(j)}\mathbf{h}_k\|^2$ has the same degrees of freedom of $N(K-k+1)$ in (47) and (48) as $||\mathbf{h}_k||^2$ by Proposition 2. Hence, their linear combination (63) behaves as $P_t^{-N(K-k+1)}$ as $P_t\to\infty$, and furthermore the term (58) as a linear combination of terms (63) behaves as $P_t^{-N(K-k+1)}$ as $P_t\to\infty$. Now, by adding (58) and the term in (51), we have the exact outage probability. We already showed that the term in (51) behaves as $P_t^{-N(K-k+1)}$ as $P_t\to\infty$. Furthermore, the upper bound of (58) behaves as $P_t^{-N(K-k+1)}$ as $P_t\to\infty$. Hence, we have $-D_k=\lim_{P_t\to\infty}\frac{\log\Pr(R_k<R^{th})}{\log P_t}\leq -N(K-k+1)$. Combining this upper bound result with the lower bound result, we have

$$N(K-k+1)\leq D_k=-\lim_{P_t\to\infty}\frac{\log\Pr(R_k<R^{th})}{\log P_t}\leq N(K-k+1). \tag{66}$$

■

Corollary 1: For the K-user Gaussian MISO BC with N transmit antennas with independent Rayleigh fading described in Section II-A, the diversity order of the overall system achievable by the proposed transceiver architecture is given by

$$D=N \tag{67}$$

Proof: The decay rate of the overall outage probability is dominated by the worst decay rate. The worst diversity order in Theorem 1 occurs when $k = K$, and is given by N. ■

Note that the diversity order of the full ZF downlink beamforming is given by [14]

$$D = N - K + 1. \tag{68}$$

Surprisingly, the proposed transceiver architecture can achieve the diversity order N of the single-user MRT transmit beamforming discussed in Section II-B! Hence, the diversity order achievable by the proposed transceiver architecture is much higher than that by the fully linear ZF downlink beamforming in the multi-user case.

Note that the proposed transceiver architecture requires channel state information at the transmitter (CSIT). However, the ZF downlink beamforming also requires CSIT. The main point here is that under channel fading environments, the proposed transceiver architecture modifies the distribution of the rate of each user so that the modified rate distribution has a much lighter lower tail than the distribution of the rate of each user resulting from the ZF beamforming. Hence, communication outage occurs with much less probability and communication is much more reliable with the proposed architecture compared to the ZF downlink beamforming for the same SNR. In real-world practical cellular systems, rate adaptation is applied based on CSIT, but power control is also applied so that the residual communication outage is maintained at a certain probability. Hence, the modified light lower tail distribution of each user rate by the proposed architecture is meaningful for real-world cellular systems.

V. Numerical results

In this section, we provide some numerical results to validate our theoretical analysis in the previous sections. We considered the K-user MISO BC described in Section II-A. In each simulation scenario, we generated the K channel vectors $\mathbf{h}_1, \cdots, \mathbf{h}_K$ of the system independently from the zero-mean complex Gaussian distribution $\mathcal{CN}(\mathbf{0}, 2\mathbf{I})$ sufficiently many times to numerically compute outage probability. For each channel realization, we ran the user grouping algorithm, Algorithm 1, with $\theta^{th} = 0.9$. With the constructed groups, we applied inter-group ZF beamforming and designed the intra-group beam vectors according to the constraint (24), i.e., $\mathbf{w}_1 = \cdots = \mathbf{w}_L = \mathbf{w}^*$ with the solution $\mathbf{w}^*$ to the max-min problem (69) used in the proof of Proposition 1. The rate R_k of the k-th user is obtained based on the designed beam vectors in this way. (Note that the beam vectors $\mathbf{w}_1 = \cdots = \mathbf{w}_L = \mathbf{w}^*$ designed in this way yield rates larger than or equal to the lower bounds in (25) and (26).) For the intra-group beam design, the power distribution factors are chosen to satisfy the condition in Lemma 4 in Appendix. The used

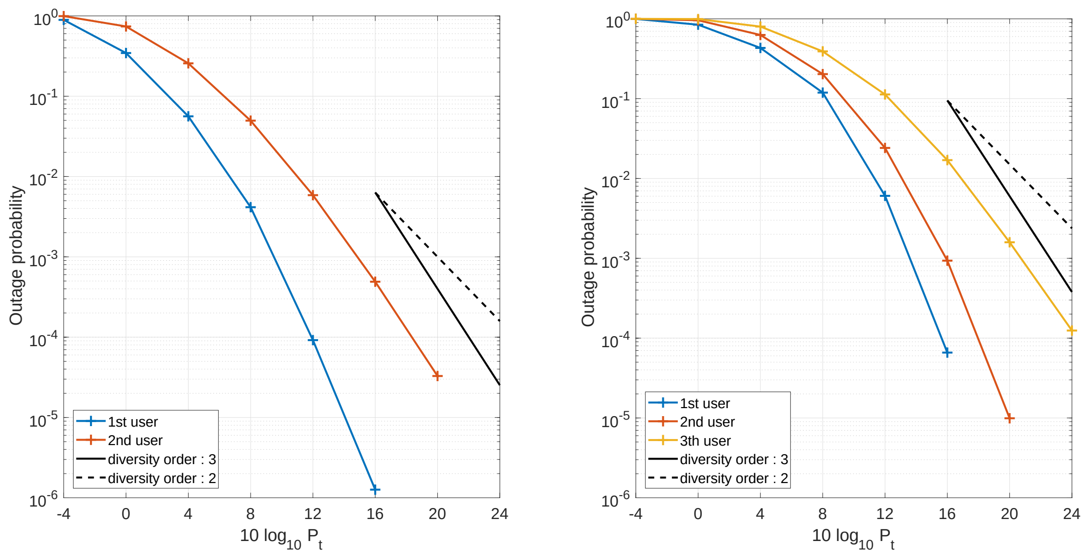

(a) (b)

Fig. 2: Outage probability of the proposed transceiver architecture: (a) $N = 3$, $K = 2$ and (b) $N = 3$, $K = 3$

values for power distribution factors are $(0.2, 0.8)$ for every two-user group, $(0.05, 0.2, 0.75)$ for every three-user group for Figs. 2(a), 2(b) and 3(a), and are the solution of (95) with $C = 2$ for Fig. 3(b). For computation of the outage probability $\Pr(R_k \leq R_{th})$, we set the target rate threshold as $R_{th} = 1.5$ [bits/channel use] through the simulations.

First, we numerically evaluated the outage probability and diversity order of each user of the proposed transceiver architecture with considering channel norm ordering. Fig. 2 shows the outage probability of the proposed new transceiver architecture in two cases: (a) $N = 3$, $K = 2$ and (b) $N = 3$ and $K = 3$, where User k is defined as the user with the k-th largest channel norm (i.e. $\|\mathbf{h}_1\|^2 \geq \|\mathbf{h}_2\|^2 \geq \cdots \geq \|\mathbf{h}_K\|^2$). In the case (a) of $N = 3, K = 2$, Theorem 1 states that the diversity orders of Users 1 and 2 are 6 and 3, respectively. It is seen in Fig. 2(a) that the outage probability of User 2 has the slope corresponding to diversity order of 3, as SNR increases. It is also seen that the decay rate of User 1 is almost twice larger than that of User 2. (In $\log_{10}$ y-scale, roughly User 1 has -4 and -5.9 and User 2 has -2.2 and -3.3 at $10 \log P_t = 12$ and 16, respectively.) In the case (b) of $N = 3,\ K = 3$, Theorem 1 states that the diversity orders of Users 1, 2 and 3 are 9, 6, and 3, respectively. It is observed in Fig. 2(b) that the outage probability of User 3 has the slope corresponding to diversity order of 3, as SNR increases.

Next, we compared the proposed new transceiver architecture with the full ZF downlink beamforming,

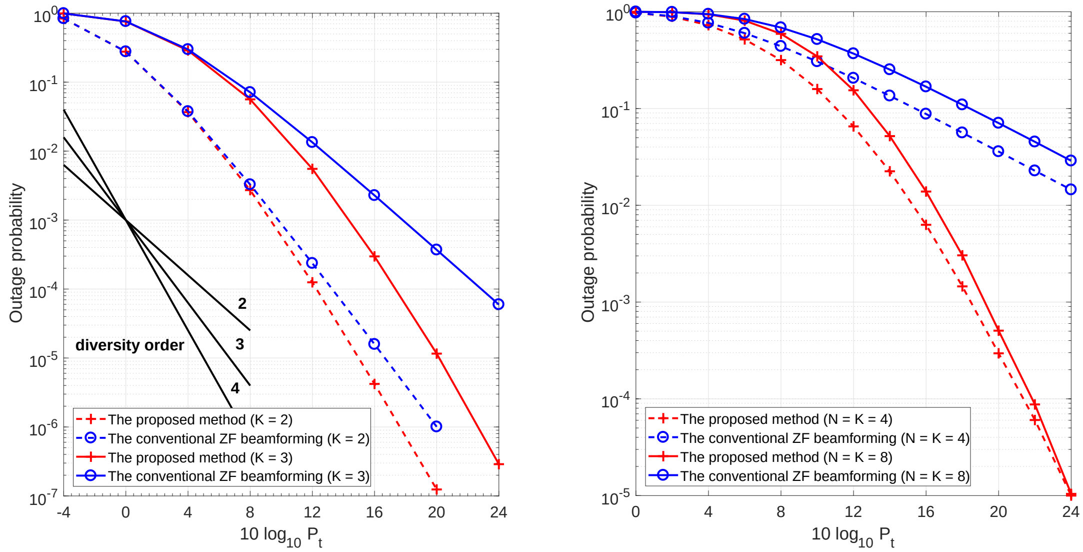

(a) (b)

Fig. 3: Overall outage probability : (a) $N = 4,\ K = 2$ or 3 and (b) $N = K = 4$ and $N = K = 8$

based on the overall system diversity order. In order to see the overall diversity order, we computed overall outage probability. For this, we neglected channel norm ordering and computed the total number of outages occurred at all K users over all Monte Carlo runs. Fig. 3 shows the overall outage probability for the same channel statistics and the same rate threshold for the proposed scheme and the ZF downlink beamforming. We considered four cases: *i)* $N = 4, K = 2$ and *ii)* $N = 4, K = 3$ shown in Fig. 3(a) and *iii)* $N = K = 4$ and *iv)* $N = K = 8$ shown in Fig. 3(b). For the considered cases *i), ii), iii),* and *iv)*, the corresponding system diversity orders of the proposed scheme are 4, 4, 4 and 8 by Corollary 1, whereas the corresponding diversity orders of the ZF downlink beamforming are 3, 2, 1, and 1 by (68). It is seen in Fig. 3(a) that indeed the diversity orders of cases *i)* and *ii)* for the proposed scheme are the same as four. (The two red curves in Fig. 3(a) seem to have the same slope with some offset, as SNR increases.) On the other hand, it is seen that the diversity orders of the ZF downlink beamforming depends on K for the same N, as expected. The outage performance result for the cases with more transmit antennas $N = K = 4$ and $N = K = 8$ is shown in Fig. 3(b). It is seen that the full ZF beamforming yields the same slope for the two cases $N = K = 4$ and $N = K = 8$, as expected, since it yields the diversity order of one in both cases by (68). On the other hand, it is seen that the diversity orders in the two cases $N = K = 4$ and $N = K = 8$ are different for the proposed scheme, as predicted by Corollary 1. Indeed, it is seen that the decay rate of the outage probability in the case of $N = K = 8$ is larger than that of the case of $N = K = 4$, although the outage probability of the case $N = K = 8$ is higher than that of the case $N = K = 4$ at low SNR. Note that the outage performance gain by the proposed scheme over the ZF beamforming is drastic in the case of full spatial multiplexing with $N = 4$ or $N = 8$ for the meaningful range where the outage probability is below 10^{-2}.

VI. Conclusion

In this paper, we have proposed a new transceiver architecture for K-user MISO BCs, based on channel-adaptive user grouping and mixture of linear and nonlinear SIC reception, and have shown that it is possible to achieve the same diversity order as that of the single-user MRT beamforming even for K-user MISO BCs under independent Rayleigh channel fading based on the proposed transceiver architecture. The proposed transceiver architecture can provide far better outage performance and more reliable communication compared to the widely-used conventional ZF downlink beamforming for MU-MISO BCs under channel fading environments. The work here is a starting point showing the promising aspect of the new mixture architecture for ultra-reliable communication in multi-user MISO downlink. Future research directions include optimization of angle threshold and power distribution by considering not only outage performance but also other metrics such as sum rate, finding faster grouping algorithms for large systems, adaptive transceiver design based on switching between the proposed architecture and ZF beamforming depending on the emphasis on diversity or sum rate, and application of the proposed architecture to the uplink.

Appendix

Proof of Proposition 1 requires the following lemma:

Lemma 2: Consider the following max-min optimization problem:

$$\begin{aligned} \max \quad & \min\left\{\left|\left(\frac{\mathbf{g}_1}{\|\mathbf{g}_1\|}\right)^H \mathbf{w}\right|^2, \cdots, \left|\left(\frac{\mathbf{g}_L}{\|\mathbf{g}_L\|}\right)^H \mathbf{w}\right|^2\right\} \\ \text{subject to} \quad & \|\mathbf{w}\|^2 \leq 1. \end{aligned} \tag{69}$$

The optimal solution $\mathbf{w}^*$ to the problem (69) satisfies the following:

$$\min\left\{\left|\left(\frac{\mathbf{g}_1}{\|\mathbf{g}_1\|}\right)^H \mathbf{w}^*\right|^2, \cdots, \left|\left(\frac{\mathbf{g}_L}{\|\mathbf{g}_L\|}\right)^H \mathbf{w}^*\right|^2\right\} \geq \frac{1}{c}, \tag{70}$$

where

$$c = \begin{cases} L & \text{if} \quad L \leq 3, \\ 8L^2 & \text{if} \quad L > 3. \end{cases} \tag{71}$$

Proof of Lemma 2: Define unit-norm $\mathbf{v}_i := \mathbf{g}_i/\|\mathbf{g}_i\|$ for $i = 1, \cdots, L$. Then, (69) can be rewritten as

$$\begin{array}{ll} \max & \min\left\{\left|\mathbf{v}_1^H\mathbf{w}\right|^2, \cdots, \left|\mathbf{v}_L^H\mathbf{w}\right|^2\right\} \\ \text{subject to} & \|\mathbf{w}\|^2 \le 1 \end{array} \tag{72}$$

The problem (72) can be reformulated as

$$\max \frac{\min\left\{\left|\mathbf{v}_1^H\mathbf{w}\right|^2, \cdots, \left|\mathbf{v}_L^H\mathbf{w}\right|^2\right\}}{||\mathbf{w}||^2} = \min \frac{||\mathbf{w}||^2}{\min\left\{\left|\mathbf{v}_1^H\mathbf{w}\right|^2, \cdots, \left|\mathbf{v}_L^H\mathbf{w}\right|^2\right\}}, \tag{73}$$

where inversion of the cost function is taken in the right-hand side (RHS) of (73) . Thus, it is known that the optimal value of the problem (72) is equivalent to the inverse of the optimal value of the following quadratic programming (QP) [21]:

$$\begin{array}{ll} \min & \|\mathbf{w}\|^2 \\ \text{subject to} & |\mathbf{v}_i^H\mathbf{w}|^2 \ge 1, \quad i = 1, \cdots, L. \end{array} \tag{74}$$

The QP (74) can be solved by semi-definite relaxation of the rewritten form of (74) [21]:

$$\begin{array}{ll} \min & \mathrm{Tr}(\mathbf{W}) \\ \text{subject to} & \mathrm{Tr}(\mathbf{V}_i\mathbf{W}) \ge 1, \quad i = 1, \cdots, L \end{array} \tag{75}$$

where $\mathbf{W} := \mathbf{w}\mathbf{w}^H$ and $\mathbf{V}_i := \mathbf{v}_i\mathbf{v}_i^H$, $i = 1 \cdots, L$. Denote the optimal values of the optimization problems (74) and (75) by v_{qp}^* and v_{sdp}^*, respectively. Then, the relationship between v_{qp}^* and v_{sdp}^* is known as [22]

$$\begin{array}{ll} v_{qp}^* = v_{sdp}^*, & \text{if} \quad L \le 3, \\ v_{qp}^* \le 8L \cdot v_{sdp}^*, & \text{if} \quad L > 3. \end{array} \tag{76}$$

Furthermore, note that $\mathbf{W}' := \sum_{i=1}^L \mathbf{V}_i$ is feasible for the problem (75) since $\mathrm{Tr}(\mathbf{V}_i\mathbf{W}') = \mathrm{Tr}(\mathbf{V}_\mathrm{i}\sum_{\mathrm{i=1}}^{\mathrm{L}}\mathbf{V}_\mathrm{i})) \ge \sum_{i=1}^L \mathrm{Tr}(\mathbf{V}_\mathrm{i}\mathbf{V}_\mathrm{i})) \ge \mathrm{Tr}(\mathbf{V}_i\mathbf{V}_i) = 1$, and $\mathrm{Tr}(\mathbf{W}') = L$. Hence, we have

$$v_{sdp}^* \le L. \tag{77}$$

Hence, with the optimal solution $\mathbf{w}^*$ to (72), we have

$$\min\left\{\left|\mathbf{v}_1^H\mathbf{w}^*\right|^2, \cdots, \left|\mathbf{v}_1^H\mathbf{w}^*\right|^2\right\} \overset{(a)}{=} 1/v_{qp}^* \overset{(b)}{\ge} L/c \cdot 1/v_{sdp}^* \overset{(c)}{\ge} 1/c, \tag{78}$$

where c is given by (71). Here, Step (a) is valid due to the relationship between the original problem (72) and the QP (74); Step (b) is valid due to (76); and Step (c) is valid due to (77). ■

Proof of Proposition 1: For given $(\delta_1, \cdots, \delta_L)$, to obtain a lower bound on the achievable rate of each user, we simply set $\mathbf{w}_1 = \mathbf{w}_2 = \cdots = \mathbf{w}_L = \mathbf{w}$ with $||\mathbf{w}||^2 \le 1$ as in the constraint (24), i.e., we consider that all L users use the same beam vector. Then, the rates in (19) and (20) of the L-user MISO BC with superposition coding and SIC can be rewritten as

$$R_1 = \log_2\left(1 + \delta_1 P|\mathbf{g}_1^H\mathbf{w}|^2\right) \tag{79}$$

$$\begin{aligned} R_i &= \log_2\left(1 + \min\left\{\frac{\delta_i P|\mathbf{g}_1^H\mathbf{w}|^2}{\sum_{m=1}^{i-1}\delta_m P|\mathbf{g}_1^H\mathbf{w}|^2 + 1}, \cdots, \frac{\delta_i P|\mathbf{g}_i^H\mathbf{w}|^2}{\sum_{m=1}^{i-1}\delta_m P|\mathbf{g}_i^H\mathbf{w}|^2 + 1}\right\}\right), \quad i = 2, \cdots, L, \\ &= \log_2\left(1 + \frac{\delta_i}{\sum_{m=1}^{i-1}\delta_m} \cdot \frac{1}{1 + 1/\left[\min\left\{|\mathbf{g}_1^H\mathbf{w}|^2, \cdots, |\mathbf{g}_i^H\mathbf{w}|^2\right\}\left(\sum_{m=1}^{i-1}\delta_m\right)P\right]}\right) \end{aligned} \tag{80}$$

Using Lemma 2, we can bound the terms $|\mathbf{g}_1^H\mathbf{w}|^2$ in (79) and $\min\left\{|\mathbf{g}_1^H\mathbf{w}|^2, \cdots, |\mathbf{g}_i^H\mathbf{w}|^2\right\}$ in (80) as follows: Using the optimal solution $\mathbf{w}^*$ to the max-min problem (69), we have

$$|\mathbf{g}_1^H\mathbf{w}^*|^2 \ge \min\left\{\left|\left(\frac{\mathbf{g}_1}{\|\mathbf{g}_1\|}\right)^H\mathbf{w}^*\right|^2, \cdots, \left|\left(\frac{\mathbf{g}_L}{\|\mathbf{g}_L\|}\right)^H\mathbf{w}^*\right|^2\right\}\|\mathbf{g}_1\|^2 \tag{81}$$

$$\ge \frac{1}{c}\|\mathbf{g}_1\|^2, \tag{82}$$

where (81) is valid since the minimum is taken over multiple terms including $|\mathbf{g}_1^H\mathbf{w}^*|^2$, and (82) is valid by Lemma 2. Next, we have

$$\min\{|\mathbf{g}_1^H\mathbf{w}^*|^2, \cdots, |\mathbf{g}_i^H\mathbf{w}^*|^2\} = \min\left\{\left|\left(\frac{\mathbf{g}_1}{\|\mathbf{g}_i\|}\right)^H\mathbf{w}^*\right|^2, \cdots, \left|\left(\frac{\mathbf{g}_i}{\|\mathbf{g}_i\|}\right)^H\mathbf{w}^*\right|^2\right\}\|\mathbf{g}_i\|^2 \tag{83}$$

$$\ge \min\left\{\left|\left(\frac{\mathbf{g}_1}{\|\mathbf{g}_1\|}\right)^H\mathbf{w}^*\right|^2, \cdots, \left|\left(\frac{\mathbf{g}_i}{\|\mathbf{g}_i\|}\right)^H\mathbf{w}^*\right|^2\right\}\|\mathbf{g}_i\|^2 \tag{84}$$

$$\ge \min\left\{\left|\left(\frac{\mathbf{g}_1}{\|\mathbf{g}_1\|}\right)^H\mathbf{w}^*\right|^2, \cdots, \left|\left(\frac{\mathbf{g}_L}{\|\mathbf{g}_L\|}\right)^H\mathbf{w}^*\right|^2\right\}\|\mathbf{g}_i\|^2 \tag{85}$$

$$\ge \frac{1}{c}\|\mathbf{g}_i\|^2, \tag{86}$$

where (84) is valid since $||\mathbf{g}_1|| \ge \cdots \ge ||\mathbf{g}_L||$, (85) is valid since we increased the number of terms in the minimization including the previous terms, and (86) holds by Lemma 2. Substituting (82) and (86) into (79) and (80), respectively, we have the rates that can be achieved by the optimal solution

$\mathbf{w}^* = \mathbf{w}_1 = \cdots = \mathbf{w}_L$ to the max-min problem (69):

$$R_1 \geq \log_2\left(1 + \frac{1}{c}\delta_1\|\mathbf{g}_1\|^2 P\right) \tag{87}$$

$$R_i \geq \log_2\left(1 + \frac{\delta_i}{\sum_{m=1}^{i-1}\delta_m}\frac{1}{1+\left(\frac{1}{c}\|\mathbf{g}_i\|^2\sum_{m=1}^{i-1}\delta_m P\right)^{-1}}\right), \quad i = 2, \cdots, L. \tag{88}$$

The considered design here of $\mathbf{w}_1 = \cdots = \mathbf{w}_L = \mathbf{w}^*$ with $||\mathbf{w}^*||^2 \leq 1$ and $p_i = \delta_i P$ with $(\delta_1, \cdots, \delta_L) \in \mathcal{D}$, i.e., (24), satisfies the original beam design constraint $(\mathbf{w}_1, \cdots, \mathbf{w}_L) \in \mathcal{W}^L$ and $p_i > 0, \forall i, \ \sum_{i=1}^L p_i = P$ in (22). Hence, the rates achieved by $\mathbf{w}_1 = \cdots = \mathbf{w}_L = \mathbf{w}^*$ with $(\delta_1, \cdots, \delta_L)$ are lower bounds on the achievable rates. ■

Proof of Lemma 1: The block matrix inversion formula is given as follows:

$$\begin{bmatrix} \mathbf{C} & \mathbf{U} \\ \mathbf{V} & \mathbf{D} \end{bmatrix} = \begin{bmatrix} \mathbf{C}^{-1} + \mathbf{C}^{-1}\mathbf{U}(\mathbf{D}-\mathbf{V}\mathbf{C}^{-1}\mathbf{U})^{-1}\mathbf{V}\mathbf{C}^{-1} & -\mathbf{C}^{-1}\mathbf{U}(\mathbf{D}-\mathbf{V}\mathbf{C}^{-1}\mathbf{U})^{-1} \\ -(\mathbf{D}-\mathbf{V}\mathbf{C}^{-1}\mathbf{U})^{-1}\mathbf{V}\mathbf{C}^{-1} & (\mathbf{D}-\mathbf{V}\mathbf{C}^{-1}\mathbf{U})^{-1} \end{bmatrix}, \tag{89}$$

which is used in Step (a) in the below. Now, we have

$$\begin{aligned}
&\mathbf{\Pi}^{\perp}_{[\mathbf{A},\mathbf{B}]} \\
&= \mathbf{I} - [\mathbf{A}\ \mathbf{B}]\begin{bmatrix} \mathbf{A}^H\mathbf{A} & \mathbf{A}^H\mathbf{B} \\ \mathbf{B}^H\mathbf{A} & \mathbf{B}^H\mathbf{B} \end{bmatrix}^{-1}\begin{bmatrix} \mathbf{A}^H \\ \mathbf{B}^H \end{bmatrix} \\
&\overset{(a)}{=} \mathbf{I} - [\mathbf{A}\ \mathbf{B}]\left[\begin{matrix} (\mathbf{A}^H\mathbf{A})^{-1} + (\mathbf{A}^H\mathbf{A})^{-1}\mathbf{A}^H\mathbf{B}(\mathbf{B}^H\mathbf{B}-\mathbf{B}^H\mathbf{A}(\mathbf{A}^H\mathbf{A})^{-1}\mathbf{A}^H\mathbf{B})^{-1}\mathbf{B}^H\mathbf{A}(\mathbf{A}^H\mathbf{A})^{-1}, \\ -(\mathbf{B}^H\mathbf{B}-\mathbf{B}^H\mathbf{A}(\mathbf{A}^H\mathbf{A})^{-1}\mathbf{A}^H\mathbf{B})^{-1}\mathbf{B}^H\mathbf{A}(\mathbf{A}^H\mathbf{A})^{-1}, \end{matrix}\right. \\
&\qquad\qquad \left.\begin{matrix} -(\mathbf{A}^H\mathbf{A})^{-1}\mathbf{A}^H\mathbf{B}(\mathbf{B}^H\mathbf{B}-\mathbf{B}^H\mathbf{A}(\mathbf{A}^H\mathbf{A})^{-1}\mathbf{A}^H\mathbf{B})^{-1} \\ (\mathbf{B}^H\mathbf{B}-\mathbf{B}^H\mathbf{A}(\mathbf{A}^H\mathbf{A})^{-1}\mathbf{A}^H\mathbf{B})^{-1} \end{matrix}\right]\begin{bmatrix} \mathbf{A}^H \\ \mathbf{B}^H \end{bmatrix} \\
&= \mathbf{I} - \mathbf{A}(\mathbf{A}^H\mathbf{A})^{-1}\mathbf{A}^H - \mathbf{A}(\mathbf{A}^H\mathbf{A})^{-1}\mathbf{A}^H\mathbf{B}(\mathbf{B}^H\mathbf{B}-\mathbf{B}^H\mathbf{A}(\mathbf{A}^H\mathbf{A})^{-1}\mathbf{A}^H\mathbf{B})^{-1}\mathbf{B}^H\mathbf{A}(\mathbf{A}^H\mathbf{A})^{-1}\mathbf{A}^H \\
&\quad + \mathbf{B}(\mathbf{B}^H\mathbf{B}-\mathbf{B}^H\mathbf{A}(\mathbf{A}^H\mathbf{A})^{-1}\mathbf{A}^H\mathbf{B})^{-1}\mathbf{B}^H\mathbf{A}(\mathbf{A}^H\mathbf{A})^{-1}\mathbf{A}^H \\
&\quad + \mathbf{A}(\mathbf{A}^H\mathbf{A})^{-1}\mathbf{A}^H\mathbf{B}(\mathbf{B}^H\mathbf{B}-\mathbf{B}^H\mathbf{A}(\mathbf{A}^H\mathbf{A})^{-1}\mathbf{A}^H\mathbf{B})^{-1}\mathbf{B}^H \\
&\quad - \mathbf{B}(\mathbf{B}^H\mathbf{B}-\mathbf{B}^H\mathbf{A}(\mathbf{A}^H\mathbf{A})^{-1}\mathbf{A}^H\mathbf{B})^{-1}\mathbf{B}^H \\
&= \mathbf{I} - \mathbf{\Pi}_{\mathbf{A}} - \mathbf{\Pi}_{\mathbf{A}}\mathbf{B}(\mathbf{B}^H\mathbf{\Pi}_{\mathbf{A}}^{\perp}\mathbf{B})^{-1}(\mathbf{\Pi}_{\mathbf{A}}\mathbf{B})^H + \mathbf{B}(\mathbf{B}^H\mathbf{\Pi}_{\mathbf{A}}^{\perp}\mathbf{B})^{-1}(\mathbf{\Pi}_{\mathbf{A}}\mathbf{B})^H \\
&\quad + \mathbf{\Pi}_{\mathbf{A}}\mathbf{B}(\mathbf{B}^H\mathbf{\Pi}_{\mathbf{A}}^{\perp}\mathbf{B})^{-1}\mathbf{B}^H - \mathbf{B}(\mathbf{B}^H\mathbf{\Pi}_{\mathbf{A}}^{\perp}\mathbf{B})^{-1}\mathbf{B}^H
\end{aligned}$$

$$= \mathbf{I} - \mathbf{\Pi}_{\mathbf{A}} - (\mathbf{B} - \mathbf{\Pi}_{\mathbf{A}}\mathbf{B})(\mathbf{B}^H\mathbf{\Pi}_{\mathbf{A}}^{\perp}\mathbf{B})^{-1}(\mathbf{B} - \mathbf{\Pi}_{\mathbf{A}}\mathbf{B})^H$$
$$= \mathbf{\Pi}_{\mathbf{A}}^{\perp} - \mathbf{\Pi}_{\mathbf{A}}^{\perp}\mathbf{B}(\mathbf{B}^H\mathbf{\Pi}_{\mathbf{A}}^{\perp}\mathbf{B})^{-1}(\mathbf{\Pi}_{\mathbf{A}}^{\perp}\mathbf{B})^H$$
$$= \mathbf{\Pi}_{\mathbf{A}}^{\perp} - \mathbf{\Pi}_{\mathbf{A}}^{\perp}\mathbf{B}((\mathbf{\Pi}_{\mathbf{A}}^{\perp}\mathbf{B})^H\mathbf{\Pi}_{\mathbf{A}}^{\perp}\mathbf{B})^{-1}(\mathbf{\Pi}_{\mathbf{A}}^{\perp}\mathbf{B})^H$$

where $\mathbf{\Pi}_{\mathbf{A}} = \mathbf{A}(\mathbf{A}^H\mathbf{A})^{-1}\mathbf{A}^H$ and $\mathbf{\Pi}_{\mathbf{A}}^{\perp} = \mathbf{I} - \mathbf{A}(\mathbf{A}^H\mathbf{A})^{-1}\mathbf{A}^H$. In the last equality, we used $\mathbf{\Pi}_{\mathbf{A}}^{\perp H}\mathbf{\Pi}_{\mathbf{A}}^{\perp} = (\mathbf{\Pi}_{\mathbf{A}}^{\perp})^2 = \mathbf{\Pi}_{\mathbf{A}}^{\perp}$. Therefore, we have

$$\mathbf{\Pi}_{[\mathbf{A},\mathbf{B}]}^{\perp}\mathbf{x} = \mathbf{\Pi}_{\mathbf{A}}^{\perp}\mathbf{x} - \mathbf{\Pi}_{\mathbf{A}}^{\perp}\mathbf{B}((\mathbf{\Pi}_{\mathbf{A}}^{\perp}\mathbf{B})^H\mathbf{\Pi}_{\mathbf{A}}^{\perp}\mathbf{B})^{-1}(\mathbf{\Pi}_{\mathbf{A}}^{\perp}\mathbf{B})^H\mathbf{x}$$
$$= \mathbf{\Pi}_{\mathbf{A}}^{\perp}\mathbf{x} - \mathbf{\Pi}_{\mathbf{A}}^{\perp}\mathbf{B}((\mathbf{\Pi}_{\mathbf{A}}^{\perp}\mathbf{B})^H\mathbf{\Pi}_{\mathbf{A}}^{\perp}\mathbf{B})^{-1}(\mathbf{\Pi}_{\mathbf{A}}^{\perp}\mathbf{B})^H(\mathbf{\Pi}_{\mathbf{A}}\mathbf{x} + \mathbf{\Pi}_{\mathbf{A}}^{\perp}\mathbf{x})$$
$$\stackrel{(b)}{=} \mathbf{\Pi}_{\mathbf{A}}^{\perp}\mathbf{x} - \mathbf{\Pi}_{\mathbf{A}}^{\perp}\mathbf{B}((\mathbf{\Pi}_{\mathbf{A}}^{\perp}\mathbf{B})^H\mathbf{\Pi}_{\mathbf{A}}^{\perp}\mathbf{B})^{-1}(\mathbf{\Pi}_{\mathbf{A}}^{\perp}\mathbf{B})^H\mathbf{\Pi}_{\mathbf{A}}^{\perp}\mathbf{x}$$
$$= (\mathbf{I} - \mathbf{\Pi}_{\mathbf{A}}^{\perp}\mathbf{B}((\mathbf{\Pi}_{\mathbf{A}}^{\perp}\mathbf{B})^H\mathbf{\Pi}_{\mathbf{A}}^{\perp}\mathbf{B})^{-1}(\mathbf{\Pi}_{\mathbf{A}}^{\perp}\mathbf{B})^H)\mathbf{\Pi}_{\mathbf{A}}^{\perp}\mathbf{x}$$
$$= (\mathbf{I} - \mathbf{\Pi}_{\mathbf{\Pi}_{\mathbf{A}}^{\perp}\mathbf{B}})\mathbf{\Pi}_{\mathbf{A}}^{\perp}\mathbf{x},$$

where Step (b) holds because $\mathbf{\Pi}_{\mathbf{A}}^{\perp}\mathbf{B}((\mathbf{\Pi}_{\mathbf{A}}^{\perp}\mathbf{B})^H\mathbf{\Pi}_{\mathbf{A}}^{\perp}\mathbf{B})^{-1}(\mathbf{\Pi}_{\mathbf{A}}^{\perp}\mathbf{B})^H$ is the projection onto $\mathcal{C}(\mathbf{\Pi}_{\mathbf{A}}^{\perp}\mathbf{B})$ which is a subspace contained in $\mathcal{C}^{\perp}(\mathbf{A})$. ■

Proof of Proposition 2: Consider the effective channel $\mathbf{g}_i^{(j)} = \mathbf{\Pi}_{\tilde{\mathbf{H}}_j}^{\perp}\mathbf{h}_i^{(j)}$, where $\mathbf{h}_i^{(j)}$ is the channel vector of User i in group $\mathcal{G}_j$, and $\tilde{\mathbf{H}}_j$ is defined in (14). By Lemma 1, $\mathbf{g}_i^{(j)} = \mathbf{\Pi}_{\tilde{\mathbf{H}}_j}^{\perp}\mathbf{h}_i^{(j)}$ can be obtained from sequentially projecting $\mathbf{h}_i^{(j)}$ onto the sequential orthogonal spaces associated with the channel vectors of $\mathcal{G}_1, \mathcal{G}_2, \cdots, \mathcal{G}_{j-1}, \mathcal{G}_{j+1}, \cdots,\ \mathcal{G}_{N_g}$, as discussed in Lemma 1 and Example 1, i.e., $\mathbf{g}_i^{(j)} = \mathcal{P}(\mathcal{G}_{N_g}|\mathcal{G}_{N_g-1}, \cdots, \mathcal{G}_{j+1}, \mathcal{G}_{j-1}, \cdots, \mathcal{G}_1)\cdots\mathcal{P}(\ \mathcal{G}_{j+1}|\ \mathcal{G}_{j-1}, \cdots, \mathcal{G}_1)\mathcal{P}(\mathcal{G}_{j-1}|\mathcal{G}_{j-2}, \cdots, \mathcal{G}_1)\cdots\cdot\mathcal{P}(\mathcal{G}_2|\mathcal{G}_1)$ $\mathcal{P}(\mathcal{G}_1)\mathbf{h}_i^{(j)}$, where $\mathcal{P}(\mathcal{B}|\mathcal{A})$ denotes the sequential projection onto the orthogonal space of the projected subspace of $\mathcal{B}$ onto $\mathcal{C}^{\perp}(\mathcal{A})$. (Please see Lemma 1 and Example 1.) Here, we have $N_g - 1$ projection stages. At each projection stage, the proposed user grouping algorithm, Algorithm 1, guarantees that norm reduction is not beyond $(1-\theta^{th})$. The norm of the ZF effective channel can be written as (see Example 1)

$$||\mathbf{g}_i^{(j)}||^2 = Y||\mathbf{h}_i^{(j)}||^2, \tag{90}$$

where the reduction gain random variable Y depends on the channels, but $(1-\theta^{th})^{K-1} =: Y^{th} \le Y \le 1$ since $N_g \le K$. By (90) and Lemma 3 in the below, we have the claim (42). ■

Lemma 3: Let X be a random variable satisfying the condition, $\lim_{x\to 0}\frac{\log \Pr(X\le x)}{\log x} = d$, and let Y be a random variable satisfying the condition, $Y^{th} \le Y \le 1$, where Y^{th} is some constant $\in (0, 1]$ and d is some positive constant. Then, the product $Z := XY$ satisfies $\lim_{z\to 0}\frac{\log \Pr(Z\le z)}{\log z} = d$.

Proof of Lemma 3:

$$\begin{aligned} & \Pr(X \le z) \ \le \ \Pr(Z \le z) \ \le \ \Pr(Y^{th} X \le z) \qquad (91) \\ \Leftrightarrow \quad & \Pr(X \le z) \ \le \ \Pr(Z \le z) \ \le \ \Pr(X \le \frac{z}{Y^{th}}) \\ \Leftrightarrow \quad & \lim_{z \to 0} \frac{\log \Pr(X \le z)}{\log z} \ \le \ \lim_{z \to 0} \frac{\log \Pr(Z \le z)}{\log z} \ \le \ \lim_{z \to 0} \frac{\log \Pr(X \le \frac{z}{Y^{th}})}{\log z} \\ \Leftrightarrow \quad & \lim_{z \to 0} \frac{\log \Pr(X \le z)}{\log z} \ \le \ \lim_{z \to 0} \frac{\log \Pr(Z \le z)}{\log z} \ \le \ \lim_{z \to 0} \frac{\log \Pr(X \le \frac{z}{Y^{th}})}{\log \frac{z}{Y^{th}}} \cdot \frac{\log \frac{z}{Y^{th}}}{\log z} \\ \Leftrightarrow \quad & d \ \le \ \lim_{z \to 0} \frac{\log \Pr(Z \le z)}{\log z} \ \le \ d, \end{aligned}$$

where (91) holds because $Y^{th} X \le Z = YX \le X$ due to $Y \in (Y^{th}, 1)$. Therefore, the claim follows. ■

Lemma 4: There always exists a collection of in-group power distribution factors $(\delta_1^{(j)}, \cdots, \delta_\ell^{(j)})$ for $\mathcal{G}_j$ with $|\mathcal{G}_j| = \ell$ such that $(\frac{\delta_i^{(j)}}{2^{R^{th}}-1} - \sum_{m=1}^{i-1} \delta_m^{(j)})$ in (65) is strictly positive for all $i = 2, \cdots, \ell$.

Proof: The condition is equivalent to the following:

$$\frac{\delta_i^{(j)}}{2^{R^{th}} - 1} - \sum_{m=1}^{i-1} \delta_m^{(j)} > 0 \quad \Leftrightarrow \quad \frac{\delta_i^{(j)}}{\sum_{m=1}^{i-1} \delta_m^{(j)}} > 2^{R^{th}} - 1, \quad i = 2, \cdots, \ell \qquad (92)$$

Consider the following recursion

$$\delta_i^{(j)} = (2^{R^{th}} - 1 + C)(\delta_1^{(j)} + \cdots + \delta_{i-1}^{(j)}), \qquad (93)$$

where $C > 0$ is an arbitrary positive constant. It is easy to see that any solution to (93) satisfies (92). Solving the recursion yields

$$\delta_i^{(j)} = \delta_1^{(j)} (2^{R^{th}} - 1 + C)(2^{R^{th}} + C)^{i-2}. \qquad (94)$$

With normalization for $\sum_{i=1}^{\ell} \delta_i^{(j)} = 1$, we have

$$\delta_1^{(j)} = \frac{1}{(2^{R^{th}} + C)^{\ell-1}}, \quad \text{and} \quad \delta_i^{(j)} = \frac{2^{R^{th}} - 1 + C}{(2^{R^{th}} + C)^{\ell-i+1}}, \quad i = 2, \cdots, \ell, \qquad (95)$$

and all $\delta_i^{(j)} \ge 0$. Hence, we have a collection of power distribution factors for the condition. ■

References

[1] N. Jindal, S. Viswanath, and A. Goldsmith, "On the duality of Gaussian multiple-access and broadcast channels,"*IEEE Trans. Inf. Theory*, vol. 50, pp. 768 - 783, May 2004.

[2] H. Weingarten, Y. Steinberg, and S. Shamai, "The capacity region of the Gaussian multiple-input multiple-output broadcast channels," *IEEE Trans. Inf. Theory*, vol. 52, pp. 3936-3964, Sep. 2009.

[3] M. Sharif and B. Hassibi, “On the capacity of MIMO broadcast channels with partial side information,” *IEEE Trans. Inf. Theory*, vol. 51, pp. 506-522, Feb. 2005.

[4] T. Yoo and A. Goldsmith, “On the optimality of multiantenna broadcast scheduling using zero-forcing beamforming,” *IEEE J. Sel. Areas in Commun.*, vol. 24, pp. 528-541, Mar. 2006.

[5] 3GPP, “Evolved universal terrestrial radio access (E-UTRA): Downlink multiple input multiple output (MIMO) enhancement for LTE-Advanced (Release 11),” *TR 36.871, V11.0.0*, 2011-2012.

[6] Q. H. Spencer, A. L. Swindlehurst, and M. Haardt, “Zero-forcing methods for downlink spatial multiplexing in multiuser MIMO channels,” *IEEE Trans. Signal Process.*, vol. 52, pp. 461 - 471, Feb. 2004.

[7] G. Lee and Y. Sung, “A new approach to user scheduling in massive multi-user MIMO broadcast channels,” *IEEE Trans. Commun.*, vol. 66, pp. 1481 - 1495, Apr. 2018.

[8] G. Lee, Y. Sung, and J. Seo, “Randomly-directional beamforming in mm-wave multi-user MISO downlink,” *IEEE Trans. Wireless Commun.*, vol. 15, pp. 1086-1100, Feb. 2016.

[9] G. Lee, Y. Sung, and M. Kountouris, “On the performance of random beamforming in sparse millimeter wave channels,” *IEEE J. Sel. Topics Signal Process.*, vol. 10, pp. 560-575, Apr. 2016.

[10] H. Huh, A. M. Tulino, and G. Caire, “Network mimo with linear zero-forcing beamforming: Large system analysis, impact of channel estimation, and reduced-complexity scheduling,” *IEEE Trans. Inf. Theory*, vol. 58, pp. 2911-2934, Dec. 2012.

[11] IEEE, “IEEE 5G and beyond technology roadmap white paper,” Oct. 2017.

[12] Y. Saito, Y. Kishiyama, A. Benjebbour, T. Nakamura, A. Li, and K. Higuchi, “Non-orthogonal multiple access (NOMA) for cellular future radio access,” in *Proc. IEEE VTC*, pp. 1-5, Jun. 2013.

[13] Y. Mao, B. Clerckx, and V. O. Li, “Rate-splitting multiple access for downlink communication systems: bridging, generalizing, and outperforming sdma and noma,” *EURASIP Journal on Wireless Communications and Networking*, vol. 2018, no. 1, p. 133, 2018.

[14] Z. Chen, Z. Ding, and X. Dai, “Beamforming for combating inter-cluster and intra-cluster interference in hybrid NOMA systems,” *IEEE Access*, vol. 4, pp. 4452 - 4463, Aug. 2016.

[15] J. Seo and Y. Sung, “A new transceiver architecture for multi-user MIMO communication based on mixture of linear and non-linear reception,” in *Proc. SPAWC*, (Sapporo, Japan), Jun. 2017.

[16] J. Kazemitabar and H. Jafarkhani, “Multiuser interference cancellation and detection for users with more than two transmit antennas,” *IEEE Trans. Commun.*, vol. 56, no. 4, pp. 574 - 583, 2008.

[17] D. Tse and P. Viswanath, *Fundamentals of Wireless Communication*. Cambridge University Press, 2005.

[18] M. F. Hanif, Z. Ding, T. Ratnarajah, and G. K. Karagiannidis, “A minorization-maximization method for optimizing sum rate in the downlink of non-orthogonal multiple access systems,” *IEEE Trans. Signal Process.*, vol. 64, no. 1, pp. 76-88, 2016.

[19] J. Seo and Y. Sung, “Beam design and user scheduling for non-orthogonal multiple access with multiple antennas based on Pareto-optimality,” *IEEE Trans. Signal Process.*, vol. 66, pp. 2876 - 2891, Jun. 2018.

[20] A. L. Yuille and A. Rangarajan, “The concave-convex procedure,” *Neural computation*, vol. 15, no. 4, pp. 915-936, 2003.

[21] N. D. Sidiropoulos, T. N. Davidson, and Z.-Q. Luo, “Transmit beamforming for physical-layer multicasting,” *IEEE Trans. Signal Process.*, vol. 54, no. 6, pp. 2239-2251, 2006.

[22] Z.-Q. Luo, N. D. Sidiropoulos, P. Tseng, and S. Zhang, “Approximation bounds for quadratic optimization with homogeneous quadratic constraints,” *SIAM Journal on optimization*, vol. 18, no. 1, pp. 1-28, 2007.